



Dielectron and heavy-quark production in inelastic and high-multiplicity proton–proton collisions at $\sqrt{s} = 13$ TeV

ALICE Collaboration*



ARTICLE INFO

Article history:

Received 23 May 2018

Received in revised form 8 October 2018

Accepted 6 November 2018

Available online 9 November 2018

Editor: M. Doser

ABSTRACT

The measurement of dielectron production is presented as a function of invariant mass and transverse momentum (p_T) at midrapidity ($|y_e| < 0.8$) in proton–proton (pp) collisions at a centre-of-mass energy of $\sqrt{s} = 13$ TeV. The contributions from light-hadron decays are calculated from their measured cross sections in pp collisions at $\sqrt{s} = 7$ TeV or 13 TeV. The remaining continuum stems from correlated semileptonic decays of heavy-flavour hadrons. Fitting the data with templates from two different MC event generators, PYTHIA and POWHEG, the charm and beauty cross sections at midrapidity are extracted for the first time at this collision energy: $d\sigma_{cc}/dy|_{y=0} = 974 \pm 138$ (stat.) ± 140 (syst.) ± 214 (BR) μb and $d\sigma_{bb}/dy|_{y=0} = 79 \pm 14$ (stat.) ± 11 (syst.) ± 5 (BR) μb using PYTHIA simulations and $d\sigma_{cc}/dy|_{y=0} = 1417 \pm 184$ (stat.) ± 204 (syst.) ± 312 (BR) μb and $d\sigma_{bb}/dy|_{y=0} = 48 \pm 14$ (stat.) ± 7 (syst.) ± 3 (BR) μb for POWHEG. These values, whose uncertainties are fully correlated between the two generators, are consistent with extrapolations from lower energies. The different results obtained with POWHEG and PYTHIA imply different kinematic correlations of the heavy-quark pairs in these two generators. Furthermore, comparisons of dielectron spectra in inelastic events and in events collected with a trigger on high charged-particle multiplicities are presented in various p_T intervals. The differences are consistent with the already measured scaling of light-hadron and open-charm production at high charged-particle multiplicity as a function of p_T . Upper limits for the contribution of virtual direct photons are extracted at 90% confidence level and found to be in agreement with pQCD calculations.

© 2018 The Author. Published by Elsevier B.V. This is an open access article under the CC BY license (<http://creativecommons.org/licenses/by/4.0/>). Funded by SCOAP³.

1. Introduction

Heavy-flavour quarks (charm and beauty) are copiously produced by inelastic partonic scatterings in high-energy proton–proton (pp) collisions at the CERN Large Hadron Collider (LHC). Their large masses (m_Q) make it possible to calculate their production cross sections with perturbative quantum chromodynamics (pQCD) [1–3]. Hence, experimental measurements of heavy-quark production provide an excellent test of pQCD in this energy regime. Flavour conservation allows heavy quarks to be only produced in pairs. Charm hadrons and their decay products reflect the initial angular correlation of the heavy-quark pairs, whereas in the case of decays of beauty hadrons the correlation is weakened due to their large masses. The contribution from the simultaneous semileptonic decays of the corresponding heavy-flavour hadron pairs dominates the dilepton yield in the intermediate mass region (IMR) $1 < m_{ee} < 3$ GeV/ c^2 . Hence, dielectron measurements can be used to study charm and beauty production.

The ALICE Collaboration has reported charm and beauty production cross section measurements at midrapidity ($|y| < 0.5$) in pp collisions at centre-of-mass energies of $\sqrt{s} = 2.76$ and 7 TeV [4–10]. The charm measurement at $\sqrt{s} = 7$ TeV is complemented by ATLAS data extending to higher transverse momentum (p_T) and $|y| < 2.1$ [11]. Furthermore, the CMS Collaboration has provided a variety of charm and bottom measurements at midrapidity at $\sqrt{s} = 2.76$, 5 and 7 TeV [12–20]. At forward rapidity ($2 < y < 5$), the LHCb Collaboration has measured charm and beauty production cross sections in pp collisions at $\sqrt{s} = 5$, 7, 8 and 13 TeV [21–24]. These results are generally in good agreement with pQCD calculations at next-to-leading order (NLO) in the strong coupling constant (α_s) with all-order resummation of the logarithms of p_T/m_Q (FONLL) [1–3]. Though the measured charm production cross sections consistently lie on the upper edge of the systematic uncertainties of the theory calculations. Recently, the ALICE Collaboration has measured the charm and beauty production cross sections in pp collisions at $\sqrt{s} = 7$ TeV using electron–positron pairs (dielectrons) from correlated semileptonic decays of heavy-flavour hadrons [25]. Such an approach was first performed by the PHENIX Collaboration in pp and d–Au collisions at $\sqrt{s_{NN}} = 200$ GeV at the Relativistic Heavy Ion Collider

* E-mail address: alice-publications@cern.ch.

(RHIC) [26–28]. These measurements have the advantage that they probe the full p_T range of heavy-quark pairs and contain complementary information about the initial correlation of charm quarks, i.e. the underlying production mechanism, which is not accessible in conventional single heavy-flavour measurements.

The measurement of direct photons, i.e. those produced in hard scatterings between incoming partons in hadronic collisions, provides another important test of pQCD. Furthermore, at $p_T < 3 \text{ GeV}/c$, where the applicability of perturbation theory may be questionable, experimental data of direct-photon production in pp collisions serve as a crucial reference to establish the presence of thermal radiation from the hot and dense medium created in heavy-ion collisions [29–32]. The measurement of real (massless) direct photons at low p_T is challenging because of the large background of hadron decay photons. This background can be largely reduced by measuring the contribution of virtual direct photons, i.e. direct e^+e^- pairs, to the dielectron invariant-mass spectrum above the π^0 mass [29,30].

Proton–proton collisions in which a large number of charged particles are produced have recently attracted the interest of the heavy-ion community [33,34]. These events exhibit features that are similar to those observed in heavy-ion collisions, e.g. collective effects, such as long-range angular correlations [35–40] or enhanced strangeness production [41]. Charged-hadron p_T spectra in pp collisions at $\sqrt{s} = 13 \text{ TeV}$ show a hardening with increasing multiplicity, an effect that arises naturally from jets [42]. Also, heavy-quark production is found to scale faster than linearly with the charged-particle multiplicity in pp collisions at $\sqrt{s} = 7 \text{ TeV}$ [43,44]. This motivates the study of dielectron production in high-multiplicity pp collisions. In the low mass region ($m_{ee} < 1 \text{ GeV}/c^2$), dielectron measurements provide further insight into possible modifications of the light vector and pseudo-scalar meson production via their resonance and/or Dalitz decays, whereas in the IMR they allow for complementary studies of the heavy-flavour production. At LHC energies, the contribution from open charm already dominates the dielectron continuum at $m_{ee} \approx 0.5 \text{ GeV}/c^2$. Moreover, if a thermalised system were created in such high-multiplicity pp collisions, a signal of thermal (virtual) photons should be present.

In this letter, first results of charm and beauty production cross sections at midrapidity in inelastic (INEL) and high-multiplicity (HM) pp collisions at $\sqrt{s} = 13 \text{ TeV}$ are reported. The paper is organised as follows: the ALICE apparatus and the data samples used in the analysis are described in Section 2, the data analysis is discussed in Section 3, Section 4 introduces the cocktail of known hadronic sources, and the results are presented and discussed in Section 5.

2. The ALICE detector and data samples

A detailed description of the ALICE apparatus and its performance can be found in [45–48]. The detectors used in this analysis are briefly described below.

Trajectories of charged particles are reconstructed in the ALICE central barrel with the Inner Tracking System (ITS) and the Time Projection Chamber (TPC) that reside within a solenoid, which provides a homogeneous magnetic field of 0.5 T along the beam direction. The ITS consists of six cylindrical layers of silicon detectors, with radial distances from the beam axis between 3.9 cm and 43 cm. The two innermost layers are equipped with Silicon Pixel Detectors (SPD), the two intermediate layers are composed of Silicon Drift Detectors, and the two outermost layers are made of Silicon Strip Detectors. The TPC, main tracking device in the ALICE central barrel, is a 5 m long cylindrical gaseous detector extending from 85 cm to 247 cm in radial direction. It provides up to

159 spacial points per track for charged-particle reconstruction and particle identification (PID) through the measurement of the specific ionisation energy loss dE/dx in the gas volume.

The PID is complemented by the Time-Of-Flight (TOF) system located at a radial distance of 3.7 m from the nominal interaction point. It measures the arrival time of particles relative to the event collision time provided by the TOF detector itself or by the T0 detectors, two arrays of Cherenkov counters located at forward rapidities [49].

Collision events are triggered by the V0 detector that comprises two plastic scintillator arrays placed on both sides of the interaction point at pseudorapidities $2.8 < \eta < 5.1$ and $-3.7 < \eta < -1.7$. The V0 is also used to reject background events like beam-gas interactions, collisions with de-bunched protons or with mechanical structures of the beam line.

The data samples used in this letter were recorded with ALICE in 2016 during the LHC pp run at $\sqrt{s} = 13 \text{ TeV}$. For the minimum-bias event trigger that is used to define the data sample for the analysis of inelastic pp collisions, coincident signals in both V0 scintillators are required to be synchronous with the beam crossing time defined by the LHC clock. Events with high charged-particle multiplicities are triggered on by additionally requiring the total signal amplitude measured in the V0 detector to exceed a certain threshold. At the analysis level, the 0.036 percentile of inelastic events with the highest V0 multiplicity (VOM) is selected to define the high-multiplicity event class. This value is low enough to avoid inefficiencies due to trigger threshold variations during data taking. Track segments reconstructed in the SPD are extrapolated back to the beam line to define the interaction vertex. Events with multiple vertices identified with the SPD are tagged as pile-up and removed from the analysis [48]. The vertex information may be improved based on the information provided by tracks reconstructed in the ITS and TPC. To assure a uniform detector coverage within $|\eta| < 0.8$, the vertex position along the beam direction is restricted to $\pm 10 \text{ cm}$ around the nominal interaction point. A total of 455×10^6 minimum-bias (MB) pp events and 79.2×10^6 high-multiplicity pp events are considered for further analysis, which corresponds to an integrated luminosity of $\mathcal{L}_{\text{int}}^{\text{MB}} = 7.87 \pm 0.40 \text{ nb}^{-1}$ and $\mathcal{L}_{\text{int}}^{\text{HM}} = 2.79 \pm 0.15 \text{ pb}^{-1}$, respectively. The luminosity determination is based on the visible cross section for the V0-based minimum-bias trigger, measured in a van der Meer scan carried out in 2015 [50]. A conservative uncertainty of 5% is assigned to this measurement, to account for possible variations of the cross section between the two data-taking periods.

3. Data analysis

Electron¹ candidates are selected from charged-particle tracks reconstructed in the ITS and TPC in the kinematic range $|\eta_e| < 0.8$ and $p_{T,e} > 0.2 \text{ GeV}/c$. Basic track quality criteria are applied, e.g. a sufficient number of space points measured in the TPC and ITS as well as a good track fit. The contribution from secondary tracks is reduced by requiring a maximum distance of closest approach (DCA) to the primary vertex in the transverse plane ($DCA_{xy} < 1.0 \text{ cm}$) and in the longitudinal direction ($DCA_z < 3.0 \text{ cm}$). To further suppress the contribution from photon conversions in the detector material, electron candidates are required to have a hit in the first SPD layer and no ITS clusters shared with other reconstructed tracks.

The electron identification is based on the complementary information provided by the TPC and TOF. The detector PID response,

¹ The term ‘electron’ is used for both electrons and positrons if not stated otherwise.

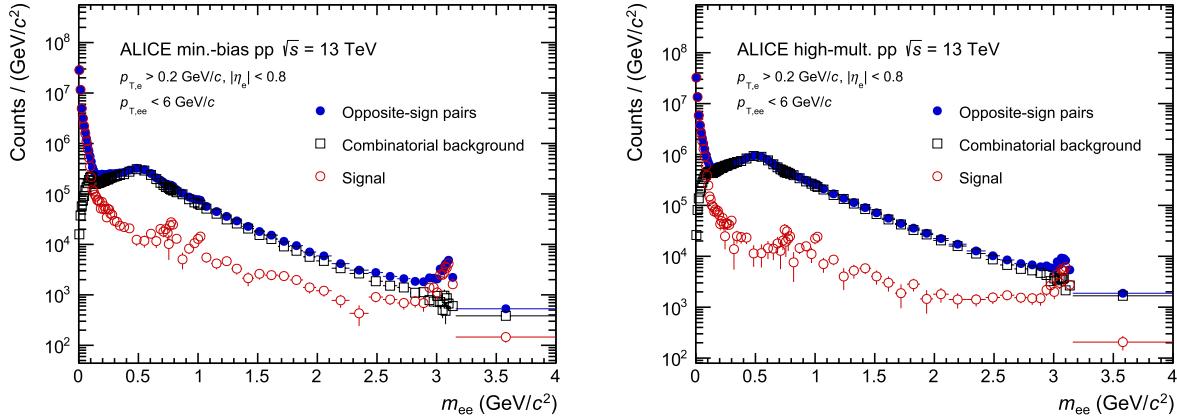


Fig. 1. Opposite-sign spectrum N_{+-} , the combinatorial background B and the signal S in minimum-bias (left) and high-multiplicity (right) events. Only statistical uncertainties are shown.

Table 1
Sources of systematic uncertainties.

Source	Minimum bias	High multiplicity
Track reconstruction	13%	13%
Electron identification	2%	2%
Conversion rejection ($m_{ee} < 0.14 \text{ GeV}/c^2$)	2%	2%
Acceptance correction factor (R)	2%	2%
Vertex distribution bias	–	6%
Multiplicity dependence of tracking and PID	–	6%
Total	14%	15%

$n(\sigma_i^{\text{DET}})$, is expressed in terms of the deviation between the measured and expected value of the specific ionisation energy loss in the TPC or time-of-flight in the TOF for a given particle hypothesis i and momentum, normalised by the detector resolution (σ_i^{DET}). In the TPC, electrons are selected in the range $|n(\sigma_e^{\text{TPC}})| < 3$ and pions are rejected by requiring $|n(\sigma_\pi^{\text{TPC}})| > 4$. Furthermore, kaons and protons are rejected with $|n(\sigma_K^{\text{TPC}})| > 4$ and $|n(\sigma_p^{\text{TPC}})| > 4$, unless the candidate is positively identified as an electron in the TOF, i.e. fulfilling $|n(\sigma_e^{\text{TOF}})| < 3$. For particles that are outside $|n(\sigma_K^{\text{TPC}})| < 4$ and $|n(\sigma_p^{\text{TPC}})| < 4$ the TOF information is only used to select electron candidates with $|n(\sigma_e^{\text{TOF}})| < 3$ if the track has an associated hit in the TOF detector.

Since experimentally the origin of each electron or positron is unknown, all electron candidates are paired considering combinations with opposite (N_{+-}) but also same-sign charge ($N_{\pm\pm}$). Most of the electron pairs arise from the combination of two electrons originating from different mother particles. These pairs give rise to the combinatorial background B that is estimated via the geometric mean of same-sign pairs $\sqrt{N_{++}N_{--}}$ within the same event. Opposite- and same-sign pairs include correlated background, e.g. originating from π^0 decays with two e^+e^- pairs in the final state ($\pi^0 \rightarrow \gamma^{(*)}\gamma^{(*)} \rightarrow e^+e^-e^+e^-$), which includes decay channels with real photons and their subsequent conversion in detector material. Such processes lead to opposite and same-sign pairs at equal rate. The background estimate needs to be corrected for the different detector acceptance of opposite and same-sign pairs. This correction factor is determined by dividing the yields of uncorrelated opposite (M_{+-}) and same-sign pairs ($M_{\pm\pm}$) in mixed events: $R = M_{+-}/(2\sqrt{M_{++}M_{--}})$. The dielectron signal is then obtained as $S = N_{+-} - B = N_{+-} - 2R\sqrt{N_{++}N_{--}}$. The signal S is shown together with the opposite-sign spectrum N_{+-} and the combinatorial background B in Fig. 1 for minimum-bias and high-multiplicity

events. In the mass interval $0.2 < m_{ee} < 3 \text{ GeV}/c^2$, the signal-to-background ratio varies in MB events between 0.3 and 0.04 with a minimum around $m_{ee} \approx 0.5 \text{ GeV}/c^2$ and is roughly constant at 0.2 in the IMR [51]. In HM events, the minimum reaches 0.01 and is about 0.08 in the IMR.

Electron–positron pairs from photon conversion in the detector material, contributing to the low mass spectrum below $0.14 \text{ GeV}/c^2$, are removed by using their distinct orientation relative to the magnetic field [25].

The data are corrected for the reconstruction efficiencies using detailed Monte Carlo (MC) simulations. For this, pp events are generated with the Monash 2013 tune of PYTHIA 8 [52] for light-hadron decays and the Perugia 2011 tune of PYTHIA 6.4 for heavy-flavour decays [53] and the resulting particles are propagated through a detector simulation using GEANT 3 [54]. The choice of the different PYTHIA versions is motivated by the fact that the Perugia 2011 tune describes reasonably well the transverse momentum spectra of heavy-flavour hadrons while the Monash 2013 tune reproduces many of the relevant light-hadron multiplicities [55,56]. The signal reconstruction efficiencies were studied as a function of m_{ee} and pair transverse momentum $p_{T,ee}$ separately for the different e^+e^- sources: resonance and Dalitz decays of relevant mesons as well as correlated semileptonic decays of charm and beauty hadrons. The total signal reconstruction efficiency is obtained by weighting the efficiency of each dielectron source by its expected contribution and is found to be about 20% in $0.7 < m_{ee} < 1.2 \text{ GeV}/c^2$ and approaches 30% at lower and higher masses.

Different aspects of the analysis are considered as possible sources of systematic uncertainties, which are summarised in Table 1. The systematic uncertainties due to the track reconstruction are estimated by comparing the efficiency of the ITS–TPC matching, the requirement of a hit in the first SPD layer, and the requirement of no shared ITS clusters in MC simulations and data. The residual disagreements between data and MC add to a 6.5% uncertainty on the single track level, which leads to a 13% uncertainty for pairs. The MC simulations were also checked to reproduce all details of the PID selection within a systematic uncertainty of 2% for e^+e^- pairs. The purity of the electron sample is estimated to be $>93\%$ over the relevant p_T range, with a p_T -integrated hadron contamination of about 4%. The resulting hadron contamination on the dielectron signal is found to be negligible. For $m_{ee} < 0.14 \text{ GeV}/c^2$, a 2% uncertainty on the conversion rejection was estimated from the yield change when tightening the selection to reject photon conversions. A 2% uncertainty on the signal yield due to the correction factor R is obtained by repeating the event mixing in different event classes, defined by the position of the reconstructed primary

vertex and by the charged-particle multiplicity. The efficiency of the minimum-bias trigger to select inelastic events with an e^+e^- pair in the ALICE acceptance ($|\eta_e| < 0.8$ and $p_{T,e} > 0.2$ GeV/c) is estimated to be $(99 \pm 1)\%$ from the Monash 2013 tune of PYTHIA 8. This and the luminosity uncertainty of 5% [50] are global uncertainties, which are not included in the point-to-point uncertainties. No significant variation of systematic uncertainties on mass or $p_{T,ee}$ is observed in the analysis, and the same total uncertainty of 14% is assigned as point-to-point correlated uncertainties on the differential dielectron cross section in inelastic pp collisions.

The analysis of the high-multiplicity data has additional systematic uncertainties. First, no dedicated high-multiplicity MC simulation was performed. In such events the vertex distribution is biased more than in MB events by the asymmetric pseudorapidity coverage of the two V0 detectors. The change of the detector acceptance with vertex position could lead to a difference in the number of reconstructed electrons of up to 3%, which results in an uncertainty of 6% for e^+e^- pairs. Second, a possible multiplicity dependence of the reconstruction and PID efficiency is covered by an uncertainty of 6% [57]. Added in quadrature, this amounts to a total uncertainty of 15%.

4. Cocktail of known hadronic sources

The dielectron spectrum measured in pp collisions at $\sqrt{s} = 13$ TeV is compared with the expectations from all known hadron sources, i.e. the hadronic cocktail, contributing to the dielectron spectrum in the ALICE central barrel acceptance ($|\eta_e| < 0.8$ and $p_{T,e} > 0.2$ GeV/c). A fast MC simulation is used to estimate the contribution from π^0 , η , η' , ρ , ω and ϕ decays in pp collisions, as detailed in [25].

Following the approach outlined in [58], the pion p_T -spectrum at $\sqrt{s} = 13$ TeV is approximated by scaling the p_T -spectrum of charged hadrons [42] by the pion-to-hadron ratio measured at $\sqrt{s} = 7$ TeV [59,60]. The difference with respect to the same procedure based on the pion-to-hadron ratio measured at $\sqrt{s} = 2.76$ TeV [59,61] is smaller than 1% at low p_T and reaches 5% at high p_T . The charged hadron p_T -spectra at $\sqrt{s} = 13$ TeV are normalised to INEL>0 events, i.e. inelastic collisions that produce at least one charged particle in $|\eta| < 1$, rather than INEL events. This is corrected taking the 21% difference in the p_T integrated $dN_{ch}/d\eta$ values for these two event classes [42]. A conservative uncertainty of 10% is assigned on this extrapolation.

A fit of the obtained charged-pion p_T -spectrum with a modified Hagedorn function is then taken as proxy for the neutral-pion p_T -distribution. The simulated cross section per unit rapidity of the π^0 is $d\sigma/dy|_{y=0} = 155.2$ mb. For the η meson a fit of the measured η/π^0 ratio in pp collisions at $\sqrt{s} = 7$ TeV is used [62]. The Monash 2013 tune of PYTHIA 8 describes the ρ/π^0 and ω/π^0 ratios measured in pp collisions at $\sqrt{s} = 2.76$ and 7 TeV, respectively [55,56]. Therefore, MC simulations obtained with this tune at $\sqrt{s} = 13$ TeV are used to obtain the ρ/π^0 and ω/π^0 ratios. Based on the η/π^0 , ρ/π^0 and ω/π^0 data, the ratios at high p_T are 0.5 ± 0.1 , 1.0 ± 0.2 and 0.85 ± 0.17 , respectively. The η' and ϕ mesons are generated assuming m_T scaling, replacing p_T with $\sqrt{m^2 - m_\pi^2 + (p_T/c)^2}$ [63]. For the m_T scaling, particle yields are normalised at high p_T relative to the π^0 yield: 0.40 ± 0.08 for η' (from PYTHIA 6 calculations) and 0.13 ± 0.04 for ϕ [64]. The detector response, including momentum and angular resolutions, as well as Bremsstrahlung effects obtained from full MC simulations, is applied to the decay electrons as a function of $p_{T,e}$, η_e and the azimuth φ_e . This results in a mass resolution of approximately 1%. The following sources of systematic uncertainties were evaluated: the input parameterisations of the measured spectra as a function of p_T (π^\pm , η/π^0 and ω/π^0), the branching fractions of all

included decay modes, the m_T scaling parameters and the resolution smearing. For the high-multiplicity cocktail, the input hadron p_T -distributions are adjusted according to the measured modifications of the charged-hadron p_T spectra [42]. The uncertainties of the cocktail from light-hadron decays are about $\pm 15\%$, reaching up to $+50\%$ in the region dominated by the η meson due to uncertainties in the extrapolation to low p_T . The multiplicity dependence has an uncertainty that varies between about 12% at low p_T and 40% at high p_T .

The Perugia 2011 tune of PYTHIA 6.4, which includes NLO parton showering processes, is used to estimate the contributions of correlated semileptonic decays of open charm and beauty hadrons [53,65]. As an alternative, the NLO event generator Powheg is also considered [66–69]. The resulting same-sign spectrum is subtracted from the opposite-sign distribution as in the data analysis. Detector effects are implemented as for the light-hadron cocktail. The spectra are normalised to cross sections at midrapidity that are based on FONLL [1–3] extrapolations of the ALICE measurements at 7 TeV [8–10]. Following the description in [70], this leads to cross sections per unit rapidity of $d\sigma_{c\bar{c}}/dy|_{y=0} = 1296^{+172}_{-162}$ μb and $d\sigma_{b\bar{b}}/dy|_{y=0} = 68^{+15}_{-16}$ μb at $\sqrt{s} = 13$ TeV. The quoted uncertainties take into account both the measured uncertainty and the FONLL extrapolation uncertainties. The latter (dominated by scale uncertainties but also including PDF and mass uncertainties) are considered to be fully correlated between the two energies [71]. For the high-multiplicity cocktail, the open charm contribution is weighted as a function of p_T according to the measured enhancement of D mesons with $p_T > 1$ GeV/c at $\sqrt{s} = 7$ TeV [43]. The same weights are applied to the open beauty contribution as no significant difference between the production of D mesons and J/ψ from beauty-hadron decays is observed [43]. For electrons originating from charm or beauty hadrons with $p_T < 1$ GeV/c, the same weight as for $1 < p_T < 2$ GeV/c is assumed in the absence of a measurement. This leads to an uncertainty on the multiplicity dependence of about 40% at low p_T decreasing to 20% at high p_T .

The J/ψ contribution is simulated with PYTHIA 6.4 and normalised to the cross section at $\sqrt{s} = 13$ TeV, extrapolated with FONLL [9] from the measurement at $\sqrt{s} = 7$ TeV by the ALICE Collaboration [72]. In the high-multiplicity cocktail, the J/ψ is scaled according to a dedicated, p_T -integrated measurement [44]. The $\psi(2S)$ contribution is normalised to the J/ψ based on a cross section ratio of $\sigma_{\psi(2S) \rightarrow e^+e^-}/\sigma_{J/\psi \rightarrow e^+e^-} = (1.59 \pm 0.17)\%$ [73].

5. Results

The dielectron cross sections are reported within the ALICE central barrel acceptance $|\eta_e| < 0.8$ and $p_{T,e} > 0.2$ GeV/c, i.e. without correction to full phase space. The result, integrated over $p_{T,ee} < 6$ GeV/c, is shown as a function of m_{ee} in the left panel of Fig. 2. The data are compared with the expectation from the hadronic decay cocktail, using PYTHIA for the heavy-flavour components, and found to be in agreement within uncertainties. Good agreement between data and cocktail calculations is also found as a function of $p_{T,ee}$, which is shown for three m_{ee} intervals in the right panel of Fig. 2.

Figs. 3 and 4 show the ratios of the dielectron spectra in high-multiplicity over inelastic events as a function of m_{ee} for different $p_{T,ee}$ intervals. To account for the trivial scaling with charged-particle multiplicity, the ratio is scaled by the factor $dN_{ch}/d\eta(\text{HM})/(dN_{ch}/d\eta(\text{INEL})) = 6.27 \pm 0.22$, where $dN_{ch}/d\eta(\text{HM}) = 33.29 \pm 0.39$ and $(dN_{ch}/d\eta(\text{INEL})) = 5.31 \pm 0.18$ are the charged-particle multiplicities in $|\eta_{ch}| < 0.5$ measured in high-multiplicity and inelastic pp collisions, respectively [42]. In this ratio, the multiplicity-independent uncertainties cancel and the total

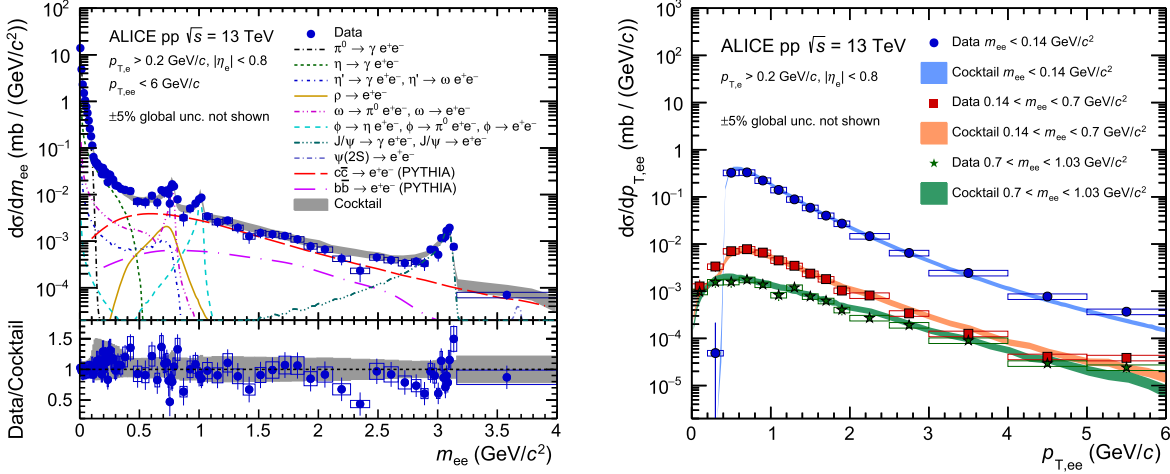


Fig. 2. The dielectron cross section in inelastic pp collisions at $\sqrt{s} = 13$ TeV as a function of invariant mass (left) and of pair transverse momentum in different mass intervals (right). The global scale uncertainty on the pp luminosity (5%) is not shown. The statistical and systematic uncertainties of the data are shown as vertical bars and boxes. The expectation from the hadronic decay cocktail is shown as a band, and the bottom left plot shows the ratio data to cocktail together with the cocktail uncertainty.

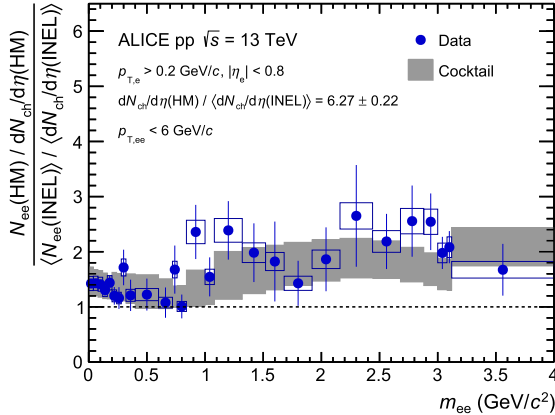


Fig. 3. Ratio of dielectron spectra in HM and INEL events scaled by the charged-particle multiplicity. The statistical and systematic uncertainties of the data are shown as vertical bars and boxes. The expectation from the hadronic decay cocktail calculation is shown as a grey band.

systematic uncertainty reduces to 9%. The ratio is in good agreement with the hadronic decay cocktail calculations over the whole measured m_{ee} and $p_{T,ee}$ range. This is the first measurement sensitive to the production of π^0 , η , ω and ϕ in high-multiplicity pp collisions. The result confirms the hypothesis that these light mesons have the same multiplicity dependence as a function of m_T , which was used in the construction of the high-multiplicity hadron cocktail. From the agreement between data and cocktail in the high- p_T range ($3 < p_{T,ee} < 6$ GeV/c), which is dominated by open beauty, it can be also concluded for the first time that the open beauty production has a multiplicity dependence similar to that of open charm. This puts additional constraints on mechanisms used to describe heavy-flavour production in high-multiplicity pp collisions, such as multiple parton interactions, percolation or hydrodynamic models.

In the intermediate mass region ($1.03 < m_{ee} < 2.86$ GeV/c²), which is dominated by open heavy-flavour decays, the data are fitted simultaneously in m_{ee} and $p_{T,ee}$ (for $p_{T,ee} < 6$ GeV/c) with PYTHIA and POWHEG templates of open charm and beauty production, keeping the light-flavour and J/ψ contributions fixed, which introduces negligible uncertainties on the heavy-flavour cross section. The PYTHIA and POWHEG least-square fits of dielectron spectra in inelastic events projected over $p_{T,ee}$ and m_{ee} are shown in the

left and right panels of Fig. 5, respectively. The resulting cross sections are summarised in Table 2. The first uncertainty is the statistical uncertainty resulting from the fits and the second is the systematic uncertainty, which is determined by moving the data points coherently upward and downward by their systematic uncertainties and repeating the fits. The branching fraction of charm-hadron decays to electrons is taken as $(9.6 \pm 0.4)\%$ [74]. An additional uncertainty of 9.3% is added in quadrature to account for differences in the Λ_c/D^0 ratio measured by ALICE in pp collisions at $\sqrt{s} = 7$ TeV, which is 0.543 ± 0.061 (stat.) ± 0.160 (syst.) for $p_T > 1$ GeV/c [75], and the LEP average of $0.113 \pm 0.013 \pm 0.006$ [76]. This translates into a 22% uncertainty at the pair level. The branching fraction of beauty hadrons decaying into electrons, including via intermediate charm hadrons, is $(21.53 \pm 0.63)\%$ [74], which leads to a 6% uncertainty on the dielectron-based cross section measurement. Like the statistical and systematic uncertainties, these branching fraction uncertainties are fully correlated between the PYTHIA and POWHEG based results.

The results are consistent with extrapolations from lower energies based on pQCD calculations discussed in the previous section. There is a strong anti-correlation between the fitted charm and beauty cross sections. The sizeable difference in the cross sections between the two MC event generators are comparable to what is observed at $\sqrt{s} = 7$ TeV [25]. The different cross sections obtained from fits with PYTHIA and POWHEG simulations are caused by acceptance differences of e^+e^- pairs from heavy-flavour hadron decays in these two event generators because of different kinematic correlations of the heavy quark pairs, in particular in rapidity. The fraction of e^+e^- pairs that fall into the ALICE acceptance and the intermediate mass region originating from $c\bar{c}$ pairs at midrapidity is 14% in PYTHIA and 10% in POWHEG. This points to important differences in the heavy quark production mechanisms between the two generators. It should be stressed that single heavy-flavour measurements appear insensitive to these differences as the cross sections obtained from such measurements agree between PYTHIA and POWHEG based extrapolations [7,11,22]. Therefore, dielectrons provide complementary information on heavy-flavour production that, if properly modelled, should lead to consistent cross sections with PYTHIA and POWHEG.

Table 2 also summarises the corresponding cross sections for the high-multiplicity data. In case of PYTHIA, the measured charm cross section translates into an enhancement of 1.86 ± 0.40 (stat.) ± 0.40 (syst.) relative to the charged-particle multiplicity increase. This is consistent with the modelled multiplicity dependence used

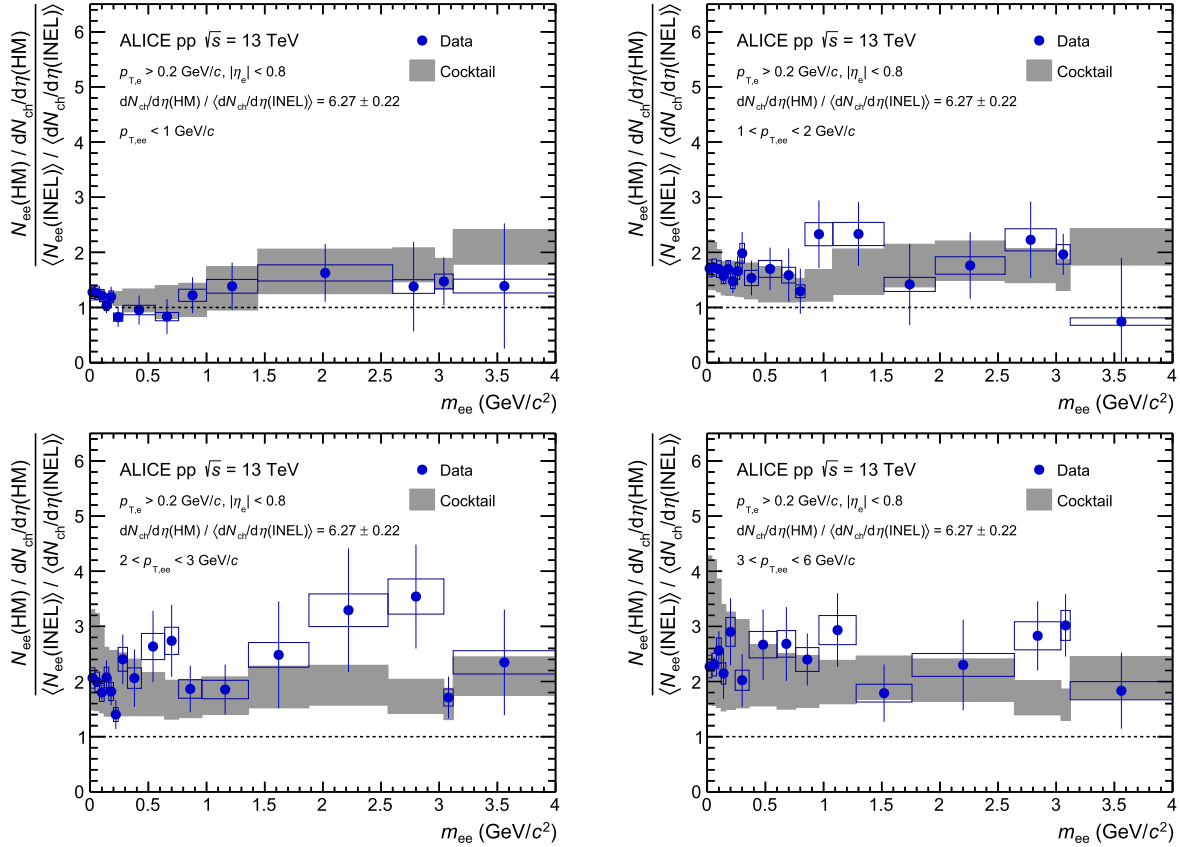


Fig. 4. Ratio of dielectron spectra in HM and INEL events scaled by the charged-particle multiplicity in different $p_{T,ee}$ intervals. The statistical and systematic uncertainties of the data are shown as vertical bars and boxes. The expectation from the hadronic decay cocktail calculation is shown as a grey band.

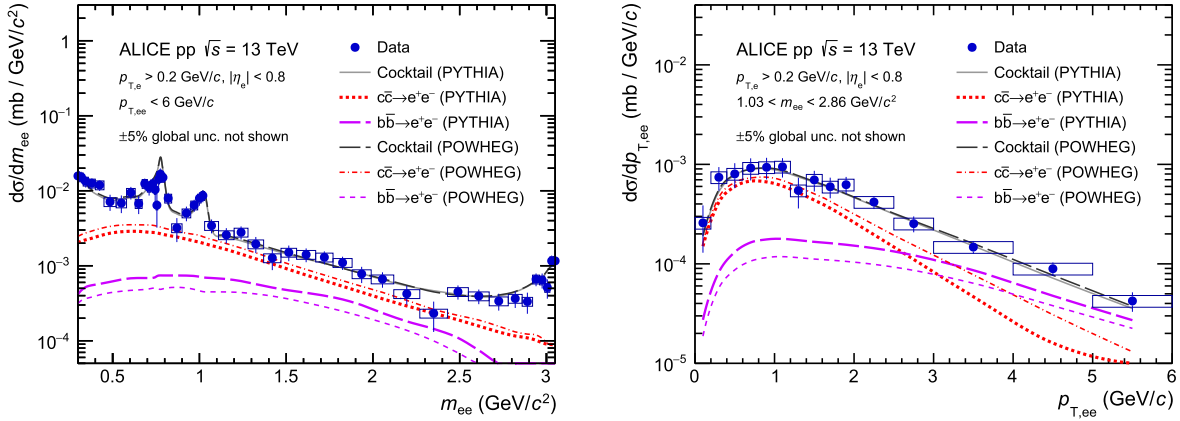


Fig. 5. Projection of the heavy-flavour dielectron fit (grey line) in inelastic pp collisions at $\sqrt{s} = 13$ TeV onto the dielectron mass (left) and $p_{T,ee}$ (right) using the PYTHIA and POWHEG event generators. The lines show the charm (red) and beauty (magenta) contributions after the fit. The global scale uncertainty on the pp luminosity (5%) is not shown. The statistical and systematic uncertainties of the data are shown as vertical bars and boxes. The fits with PYTHIA and POWHEG result in a χ^2/ndf of 57.8/66 and 52.6/66, respectively.

as input for the cocktail in Figs. 3 and 4. For the beauty cross section the observed enhancement is $1.63 \pm 0.50\text{(stat.)} \pm 0.35\text{(syst.)}$. This is consistent with the multiplicity dependence observed for open charm, but a scaling with charged-particle multiplicity cannot be excluded.

The fraction of real direct photons to inclusive photons can be extracted from the dielectron spectrum at small invariant masses assuming the equivalence between this fraction and the ratio of virtual direct photons to inclusive photons. The data are fitted minimising the χ^2 , in bins of $p_{T,ee}$, with the sum of the light-flavour cocktail ($f_{LF}(m_{ee})$), open heavy-flavour contribution

($f_{HF}(m_{ee})$) and a virtual direct photon component ($f_{direct}(m_{ee})$), whose shape is described by the Kroll–Wada equation [77,78] in the quasi-real virtual photon regime ($p_{T,ee} \gg m_{ee}$). The normalisation of the open heavy-flavour component is fixed to the measured open charm and beauty cross sections presented above, using the PYTHIA simulations for the nominal fit. As systematic uncertainty estimate, the Powheg simulation is used instead. The light-flavour cocktail and virtual direct photon templates are normalised independently to the data in $m_{ee} < 0.04$ GeV/c^2 , i.e. in a mass window in which both Dalitz decays and direct photons have the same $1/m_{ee}$ dependence. The direct-photon frac-

Table 2

Heavy-flavour cross sections in inelastic and high-multiplicity pp collisions at $\sqrt{s} = 13$ TeV. The 22% (6%) branching fraction uncertainty for charm (beauty) decays into electrons is not listed. Like statistical and systematic uncertainties, it is fully correlated between the PYTHIA and POWHEG based results.

	PYTHIA	POWHEG
$d\sigma_{cc}/dy _{y=0}$	974 ± 138 (stat.) ± 140 (syst.) μb	1417 ± 184 (stat.) ± 204 (syst.) μb
$d\sigma_{bb}/dy _{y=0}$	79 ± 14 (stat.) ± 11 (syst.) μb	48 ± 14 (stat.) ± 7 (syst.) μb
$d\sigma_{cc}/dy _{y=0}^{\text{HM}}$	4.14 ± 0.67 (stat.) ± 0.66 (syst.) μb	5.95 ± 0.91 (stat.) ± 0.95 (syst.) μb
$d\sigma_{bb}/dy _{y=0}^{\text{HM}}$	0.29 ± 0.07 (stat.) ± 0.05 (syst.) μb	0.17 ± 0.07 (stat.) ± 0.03 (syst.) μb

Table 3

Upper limits at 90% C.L. on the direct-photon fractions in comparison with the expectation in inelastic pp collisions based on a NLO pQCD calculation for a factorisation and renormalisation scale choice of $\mu = p_T$ [80].

Data sample	$1 < p_T, ee < 2$ GeV/c	$2 < p_T, ee < 3$ GeV/c	$3 < p_T, ee < 6$ GeV/c
Minimum bias	0.057	0.072	0.023
High multiplicity	0.060	0.083	0.055
pQCD	0.003	0.007	0.013

tion r is then extracted by fitting the data in the mass interval $0.14 < m_{ee} < 0.32$ GeV/c 2 , i.e. above the π^0 mass to suppress the most dominant hadron background, with the following expression: $d\sigma/dm_{ee} = r f_{\text{dir}}(m_{ee}) + (1 - r) f_{\text{LF}}(m_{ee}) + f_{\text{HF}}(m_{ee})$.

No significant direct photon contribution is observed in neither the inelastic nor the high-multiplicity events [51]. Upper limits at 90% confidence level (C.L.) are extracted with the Feldman–Cousins method [79] and summarised in Table 3 together with predictions from perturbative QCD calculations for inelastic events [80]. The current uncertainties prevent any conclusions on the scaling of direct-photon production with charged-particle multiplicity.

6. Summary and conclusion

We have presented the first measurement of dielectron production at midrapidity ($|y_e| < 0.8$) in proton–proton collisions at $\sqrt{s} = 13$ TeV. The dielectron continuum can be well described by the expected contributions from decays of light- and heavy-flavour hadrons. The charm and beauty cross sections are extracted for the first time at midrapidity at $\sqrt{s} = 13$ TeV and are consistent with extrapolations from lower energies based on pQCD calculations. The differences observed between Powheg and PYTHIA imply different kinematic correlations of the heavy-quark pairs in these two event generators. Therefore dielectrons are uniquely sensitive to the heavy quark production mechanisms. The comparison of the dielectron spectra in inelastic events and in events with high charged-particle multiplicities does not reveal modifications of the spectrum beyond the already established ones of light and open charm hadrons. The upper limits on the direct-photon fractions are consistent with predictions from perturbative quantum chromodynamics calculations.

Acknowledgements

The ALICE Collaboration would like to thank Werner Vogelsang for providing the NLO pQCD calculations for direct photon production.

The ALICE Collaboration would like to thank all its engineers and technicians for their invaluable contributions to the construction of the experiment and the CERN accelerator teams for the outstanding performance of the LHC complex. The ALICE Collaboration gratefully acknowledges the resources and support provided by all Grid centres and the Worldwide LHC Computing Grid (WLCG),

collaboration. The ALICE Collaboration acknowledges the following funding agencies for their support in building and running the ALICE detector: A. I. Alikhanyan National Science Laboratory (Yerevan Physics Institute) Foundation (ANSL), State Committee of Science and World Federation of Scientists (WFS), Armenia; Austrian Academy of Sciences and Nationalstiftung für Forschung, Technologie und Entwicklung, Austria; Ministry of Communications and High Technologies, National Nuclear Research Center, Azerbaijan; Conselho Nacional de Desenvolvimento Científico e Tecnológico (CNPq), Universidade Federal do Rio Grande do Sul (UFRGS), Financiadora de Estudos e Projetos (Finep) and Fundação de Amparo à Pesquisa do Estado de São Paulo (FAPESP), Brazil; Ministry of Science & Technology of China (MSTC), National Natural Science Foundation of China (NSFC) and Ministry of Education of China (MOEC), China; Ministry of Science and Education, Croatia; Ministry of Education, Youth and Sports of the Czech Republic, Czech Republic; The Danish Council for Independent Research Natural Sciences, the Carlsberg Foundation and Danish National Research Foundation (DNRF), Denmark; Helsinki Institute of Physics (HIP), Finland; Commissariat à l’Énergie Atomique (CEA) and Institut National de Physique Nucléaire et de Physique des Particules (IN2P3) and Centre National de la Recherche Scientifique (CNRS), France; Bundesministerium für Bildung, Wissenschaft, Forschung und Technologie (BMBF) and GSI Helmholtzzentrum für Schwerionenforschung GmbH, Germany; General Secretariat for Research and Technology, Ministry of Education, Research and Religions, Greece; National Research, Development and Innovation Office, Hungary; Department of Atomic Energy, Government of India (DAE), Department of Science and Technology, Government of India (DST), University Grants Commission, Government of India (UGC) and Council of Scientific and Industrial Research (CSIR), India; Indonesian Institute of Sciences, Indonesia; Centro Fermi – Museo Storico della Fisica e Centro Studi e Ricerche Enrico Fermi and Istituto Nazionale di Fisica Nucleare (INFN), Italy; Institute for Innovative Science and Technology, Nagasaki Institute of Applied Science (IIIST), Japan Society for the Promotion of Science (JSPS) KAKENHI and Japanese Ministry of Education, Culture, Sports, Science and Technology (MEXT), Japan; Consejo Nacional de Ciencia (CONACYT) y Tecnología, through Fondo de Cooperación Internacional en Ciencia y Tecnología (FONCICYT) and Dirección General de Asuntos del Personal Académico (DGAPA), Mexico; Nederlandse Organisatie voor Wetenschappelijk Onderzoek (NWO), Netherlands; The Research Council of Norway, Norway; Commission on Science and Technology for Sustainable Development in the South (COMSATS), Pakistan; Pontificia Universidad Católica del Perú, Peru; Ministry of Science and Higher Education and National Science Centre, Poland; Korea Institute of Science and Technology Information and National Research Foundation of Korea (NRF), Republic of Korea; Ministry of Education and Scientific Research, Institute of Atomic Physics and Romanian National Agency for Science, Technology and Innovation, Romania; Joint Institute for Nuclear Research (JINR), Ministry of Education and Science of the Russian Federation and National Research Centre Kurchatov Institute, Russia; Ministry of Education,

Science, Research and Sport of the Slovak Republic, Slovakia; National Research Foundation of South Africa, South Africa; Centro de Aplicaciones Tecnológicas y Desarrollo Nuclear (CEADEN), Cuba-energía, Cuba and Centro de Investigaciones Energéticas, Medioambientales y Tecnológicas (CIEMAT), Spain; Swedish Research Council (VR) and Knut & Alice Wallenberg Foundation (KAW), Sweden; European Organization for Nuclear Research, Switzerland; National Science and Technology Development Agency (NSDTA), Suranaree University of Technology (SUT) and Office of the Higher Education Commission under NRU project of Thailand, Thailand; Turkish Atomic Energy Agency (TAEK), Turkey; National Academy of Sciences of Ukraine, Ukraine; Science and Technology Facilities Council (STFC), United Kingdom; National Science Foundation of the United States of America (NSF) and U.S. Department of Energy, Office of Nuclear Physics (DOE NP), United States of America.

References

- [1] M. Cacciari, M. Greco, P. Nason, The p_T spectrum in heavy flavor hadroproduction, *J. High Energy Phys.* 05 (1998) 007, arXiv:hep-ph/9803400 [hep-ph].
- [2] M. Cacciari, S. Frixione, P. Nason, The p_T spectrum in heavy flavor photoproduction, *J. High Energy Phys.* 03 (2001) 006, arXiv:hep-ph/0102134 [hep-ph].
- [3] M. Cacciari, S. Frixione, N. Houdeau, M.L. Mangano, P. Nason, G. Ridolfi, Theoretical predictions for charm and bottom production at the LHC, *J. High Energy Phys.* 10 (2012) 137, arXiv:1205.6344 [hep-ph].
- [4] ALICE Collaboration, B. Abelev, et al., Measurement of charm production at central rapidity in proton–proton collisions at $\sqrt{s} = 2.76$ TeV, *J. High Energy Phys.* 07 (2012) 191, arXiv:1205.4007 [hep-ex].
- [5] ALICE Collaboration, B. Abelev, et al., Beauty production in pp collisions at $\sqrt{s} = 2.76$ TeV measured via semi-electronic decays, *Phys. Lett. B* 738 (2014) 97, arXiv:1405.4144 [nucl-ex], Erratum: *Phys. Lett. B* 763 (2016) 507.
- [6] ALICE Collaboration, B. Abelev, et al., Measurement of electrons from semileptonic heavy-flavor hadron decays in pp collisions at $\sqrt{s} = 2.76$ TeV, *Phys. Rev. D* 91 (2015) 012001, arXiv:1405.4117 [nucl-ex].
- [7] ALICE Collaboration, J. Adam, et al., D-meson production in p–Pb collisions at $\sqrt{s_{NN}} = 5.02$ TeV and in pp collisions at $\sqrt{s} = 7$ TeV, *Phys. Rev. C* 94 (2016) 054908, arXiv:1605.07569 [nucl-ex].
- [8] ALICE Collaboration, S. Acharya, et al., Measurement of D-meson production at mid-rapidity in pp collisions at $\sqrt{s} = 7$ TeV, *Eur. Phys. J. C* 77 (2017) 550, arXiv:1702.00766 [hep-ex].
- [9] ALICE Collaboration, B. Abelev, et al., Measurement of prompt J/ψ and beauty hadron production cross sections at mid-rapidity in pp collisions at $\sqrt{s} = 7$ TeV, *J. High Energy Phys.* 11 (2012) 065, arXiv:1205.5880 [hep-ex].
- [10] ALICE Collaboration, B. Abelev, et al., Measurement of electrons from beauty hadron decays in pp collisions at $\sqrt{s} = 7$ TeV, *Phys. Lett. B* 721 (2013) 13, arXiv:1208.1902 [hep-ex], Erratum: *Phys. Lett. B* 763 (2016) 507.
- [11] ATLAS Collaboration, G. Aad, et al., Measurement of $D^{*\pm}$, D^\pm and D_s^\pm meson production cross sections in pp collisions at $\sqrt{s} = 7$ TeV with the ATLAS detector, *Nucl. Phys. B* 907 (2016) 717, arXiv:1512.02913 [hep-ex].
- [12] CMS Collaboration, V. Khachatryan, et al., Measurement of the B^+ production cross section in pp collisions at $\sqrt{s} = 7$ TeV, *Phys. Rev. Lett.* 106 (2011) 112001, arXiv:1101.0131 [hep-ex].
- [13] CMS Collaboration, V. Khachatryan, et al., Inclusive b-hadron production cross section with muons in pp collisions at $\sqrt{s} = 7$ TeV, *J. High Energy Phys.* 03 (2011) 090, arXiv:1101.3512 [hep-ex].
- [14] CMS Collaboration, S. Chatrchyan, et al., Measurement of the B^0 production cross section in pp collisions at $\sqrt{s} = 7$ TeV, *Phys. Rev. Lett.* 106 (2011) 252001, arXiv:1104.2892 [hep-ex].
- [15] CMS Collaboration, S. Chatrchyan, et al., J/ψ and $\psi(2S)$ production in pp collisions at $\sqrt{s} = 7$ TeV, *J. High Energy Phys.* 02 (2012) 011, arXiv:1111.1557 [hep-ex].
- [16] CMS Collaboration, S. Chatrchyan, et al., Suppression of non-prompt J/ψ , prompt J/ψ , and $\Upsilon(1S)$ in Pb–Pb collisions at $\sqrt{s_{NN}} = 2.76$ TeV, *J. High Energy Phys.* 05 (2012) 063, arXiv:1201.5069 [nucl-ex].
- [17] CMS Collaboration, S. Chatrchyan, et al., Measurement of the cross section for production of $b\bar{b}X$, decaying to muons in pp collisions at $\sqrt{s} = 7$ TeV, *J. High Energy Phys.* 06 (2012) 110, arXiv:1203.3458 [hep-ex].
- [18] CMS Collaboration, A.M. Sirunyan, et al., Measurement of the B^\pm meson nuclear modification factor in Pb–Pb collisions at $\sqrt{s_{NN}} = 5.02$ TeV, *Phys. Rev. Lett.* 119 (2017) 152301, arXiv:1705.04727 [hep-ex].
- [19] CMS Collaboration, A.M. Sirunyan, et al., Nuclear modification factor of D^0 mesons in Pb–Pb collisions at $\sqrt{s_{NN}} = 5.02$ TeV, *Phys. Lett. B* 782 (2018) 474, <https://doi.org/10.1016/j.physletb.2018.05.074>, arXiv:1708.04962 [nucl-ex].
- [20] CMS Collaboration, A.M. Sirunyan, et al., Measurement of prompt and non-prompt charmonium suppression in Pb–Pb collisions at 5.02 TeV, *Eur. Phys. J. C* 78 (6) (2018), arXiv:1712.08959 [nucl-ex].
- [21] LHCb Collaboration, R. Aaij, et al., Production of J/ψ and Υ mesons in pp collisions at $\sqrt{s} = 8$ TeV, *J. High Energy Phys.* 06 (2013) 064, arXiv:1304.6977 [hep-ex].
- [22] LHCb Collaboration, R. Aaij, et al., Measurements of prompt charm production cross-sections in pp collisions at $\sqrt{s} = 13$ TeV, *J. High Energy Phys.* 03 (2016) 159, arXiv:1510.01707 [hep-ex], Errata: *J. High Energy Phys.* 05 (2017) 074.
- [23] LHCb Collaboration, R. Aaij, et al., Measurements of prompt charm production cross-sections in pp collisions at $\sqrt{s} = 5$ TeV, *J. High Energy Phys.* 06 (2017) 147, arXiv:1610.02230 [hep-ex].
- [24] LHCb Collaboration, R. Aaij, et al., Measurement of the b-quark production cross-section in 7 and 13 TeV pp collisions, *Phys. Rev. Lett.* 118 (2017) 052002, arXiv:1612.05140 [hep-ex], Erratum: *Phys. Rev. Lett.* 119 (2017) 169901.
- [25] ALICE Collaboration, S. Acharya, et al., Dielectron production in proton–proton collisions at $\sqrt{s} = 7$ TeV, *J. High Energy Phys.* 09 (2018) 064, [https://doi.org/10.1007/JHEP09\(2018\)064](https://doi.org/10.1007/JHEP09(2018)064), arXiv:1805.04391 [hep-ex].
- [26] PHENIX Collaboration, A. Adare, et al., Dilepton mass spectra in pp collisions at $\sqrt{s} = 200$ GeV and the contribution from open charm, *Phys. Lett. B* 670 (2009) 313, arXiv:0802.0050 [hep-ex].
- [27] PHENIX Collaboration, A. Adare, et al., Cross section for $b\bar{b}$ production via dileptons in d–Au collisions at $\sqrt{s_{NN}} = 200$ GeV, *Phys. Rev. C* 91 (2015) 014907, arXiv:1405.4004 [nucl-ex].
- [28] PHENIX Collaboration, A. Adare, et al., Measurements of e^+e^- pairs from open heavy flavor in pp and dA collisions at $\sqrt{s_{NN}} = 200$ GeV, *Phys. Rev. C* 96 (2017) 024907, arXiv:1702.01084 [nucl-ex].
- [29] PHENIX Collaboration, A. Adare, et al., Enhanced production of direct photons in Au–Au collisions at $\sqrt{s_{NN}} = 200$ GeV and implications for the initial temperature, *Phys. Rev. Lett.* 104 (2010) 132301, arXiv:0804.4168 [nucl-ex].
- [30] STAR Collaboration, L. Adamczyk, et al., Direct virtual photon production in Au–Au collisions at $\sqrt{s_{NN}} = 200$ GeV, *Phys. Lett. B* 770 (2017) 451, arXiv:1607.01447 [nucl-ex].
- [31] ALICE Collaboration, J. Adam, et al., Direct photon production in Pb–Pb collisions at $\sqrt{s_{NN}} = 2.76$ TeV, *Phys. Lett. B* 754 (2016) 235, arXiv:1509.07324 [nucl-ex].
- [32] ALICE Collaboration, S. Acharya, et al., Direct photon production at low transverse momentum in pp collisions at $\sqrt{s} = 2.76$ and 8 TeV, arXiv:1803.09857 [nucl-ex].
- [33] C. Loizides, Experimental overview on small collision systems at the LHC, *Nucl. Phys. A* 956 (2016) 200, <https://doi.org/10.1016/j.nuclphysa.2016.04.022>, arXiv:1602.09138 [nucl-ex].
- [34] J.L. Nagle, W.A. Zajc, Small system collectivity in relativistic hadron and nuclear collisions, *Annu. Rev. Nucl. Part. Sci.* 68 (2018) 211, <https://doi.org/10.1146/annurev-nucl-101916-123209>, arXiv:1801.03477 [nucl-ex].
- [35] CMS Collaboration, V. Khachatryan, et al., Observation of long-range near-side angular correlations in pp collisions at the LHC, *J. High Energy Phys.* 09 (2010) 091, arXiv:1009.4122 [hep-ex].
- [36] CMS Collaboration, V. Khachatryan, et al., Evidence for collectivity in pp collisions at the LHC, *Phys. Lett. B* 765 (2017) 193, arXiv:1606.06198 [nucl-ex].
- [37] ALICE Collaboration, B. Abelev, et al., Multiplicity dependence of two-particle azimuthal correlations in pp collisions at the LHC, *J. High Energy Phys.* 09 (2013) 049, arXiv:1307.1249 [nucl-ex].
- [38] ATLAS Collaboration, G. Aad, et al., Observation of long-range elliptic azimuthal anisotropies in $\sqrt{s} = 13$ and 2.76 TeV pp collisions with the ATLAS detector, *Phys. Rev. Lett.* 116 (2016) 172301, arXiv:1509.04776 [hep-ex].
- [39] ATLAS Collaboration, M. Aaboud, et al., Measurements of long-range azimuthal anisotropies and associated Fourier coefficients for pp collisions at $\sqrt{s} = 5.02$ and 13 TeV and p–Pb collisions at $\sqrt{s_{NN}} = 5.02$ TeV with the ATLAS detector, *Phys. Rev. C* 96 (2017) 024908, arXiv:1609.06213 [nucl-ex].
- [40] ATLAS Collaboration, M. Aaboud, et al., Measurement of multi-particle azimuthal correlations in pp, p–Pb and low-multiplicity Pb–Pb collisions with the ATLAS detector, *Eur. Phys. J. C* 77 (2017) 428, arXiv:1705.04176 [hep-ex].
- [41] ALICE Collaboration, J. Adam, et al., Enhanced production of multi-strange hadrons in high-multiplicity pp collisions, *Nat. Phys.* 13 (2017) 535, arXiv:1606.07424 [nucl-ex].
- [42] ALICE Collaboration, J. Adam, et al., Pseudorapidity and transverse-momentum distributions of charged particles in pp collisions at $\sqrt{s} = 13$ TeV, *Phys. Lett. B* 753 (2016) 319, arXiv:1509.08734 [nucl-ex].
- [43] ALICE Collaboration, J. Adam, et al., Measurement of charm and beauty production at central rapidity versus charged-particle multiplicity in pp collisions at $\sqrt{s} = 7$ TeV, *J. High Energy Phys.* 09 (2015) 148, arXiv:1505.00664 [nucl-ex].
- [44] ALICE Collaboration, B. Abelev, et al., J/ψ production as a function of charged particle multiplicity in pp collisions at $\sqrt{s} = 7$ TeV, *Phys. Lett. B* 712 (2012) 165, arXiv:1202.2816 [hep-ex].
- [45] ALICE Collaboration, P. Cortese, et al., ALICE: Physics Performance Report, Volume I, *J. Phys. G* 30 (2004) 1517.
- [46] ALICE Collaboration, C.W. Fabjan, et al., ALICE: Physics Performance Report, Volume II, *J. Phys. G* 32 (2006) 1295.
- [47] ALICE Collaboration, K. Aamodt, et al., The ALICE experiment at the CERN LHC, *J. Instrum.* 3 (2008) S08002.

- [48] ALICE Collaboration, B. Abelev, et al., Performance of the ALICE Experiment at the CERN LHC, *Int. J. Mod. Phys. A* 29 (2014) 1430044, arXiv:1402.4476 [nucl-ex].
- [49] ALICE Collaboration, J. Adam, et al., Determination of the event collision time with the ALICE detector at the LHC, *Eur. Phys. J. Plus* 132 (2017), arXiv:1610.03055 [physics.ins-det].
- [50] ALICE Collaboration, ALICE luminosity determination for pp collisions at $\sqrt{s} = 13$ TeV, ALICE-PUBLIC-2016-002, <http://cds.cern.ch/record/2160174>, June 2016.
- [51] ALICE Collaboration, Supplemental figures: “Dielectron and heavy-quark production in inelastic and high-multiplicity proton–proton collisions at $\sqrt{s} = 13$ TeV”, ALICE-PUBLIC-2018-009, <https://cds.cern.ch/record/2317190>, May 2018.
- [52] P. Skands, S. Carrazza, J. Rojo, Tuning PYTHIA 8.1: the Monash 2013 Tune, *Eur. Phys. J. C* 74 (2014) 3024, arXiv:1404.5630 [hep-ph].
- [53] T. Sjostrand, S. Mrenna, P.Z. Skands, PYTHIA 6.4 physics and manual, *J. High Energy Phys.* 05 (2006) 026, arXiv:hep-ph/0603175 [hep-ph].
- [54] R. Brun, R. Hagelberg, M. Hansroul, J.C. Lassalle, Simulation program for particle physics experiments, GEANT: User guide and reference manual, CERN, Geneva, 1978, <https://cds.cern.ch/record/118715>.
- [55] ALICE Collaboration, S. Acharya, et al., Production of the $\rho(770)^0$ meson in pp and Pb–Pb collisions at $\sqrt{s_{NN}} = 2.76$ TeV, arXiv:1805.04365 [nucl-ex].
- [56] ALICE Collaboration, Production of $\omega(782)$ in pp collisions at $\sqrt{s} = 7$ TeV, ALICE-PUBLIC-2018-004, <https://cds.cern.ch/record/2316785>, May 2018.
- [57] ALICE Collaboration, B. Abelev, et al., Multiplicity dependence of pion, kaon, proton and lambda production in p–Pb collisions at $\sqrt{s_{NN}} = 5.02$ TeV, *Phys. Lett. B* 728 (2014), arXiv:1307.6796 [nucl-ex].
- [58] ALICE Collaboration, S. Acharya, et al., Transverse momentum spectra and nuclear modification factors of charged particles in pp, p–Pb and Pb–Pb collisions at the LHC, arXiv:1802.09145 [nucl-ex].
- [59] ALICE Collaboration, B. Abelev, et al., Energy dependence of the transverse momentum distributions of charged particles in pp collisions measured by ALICE, *Eur. Phys. J. C* 73 (2013) 2662, arXiv:1307.1093 [nucl-ex].
- [60] ALICE Collaboration, J. Adam, et al., Multiplicity dependence of charged pion, kaon, and (anti)proton production at large transverse momentum in p–Pb collisions at $\sqrt{s_{NN}} = 5.02$ TeV, *Phys. Lett. B* 760 (2016) 720, arXiv:1601.03658 [nucl-ex].
- [61] ALICE Collaboration, B. Abelev, et al., Production of charged pions, kaons and protons at large transverse momenta in pp and Pb–Pb collisions at $\sqrt{s_{NN}} = 2.76$ TeV, *Phys. Lett. B* 736 (2014) 196, arXiv:1401.1250 [nucl-ex].
- [62] ALICE Collaboration, B. Abelev, et al., Neutral pion and η meson production in pp collisions at $\sqrt{s} = 0.9$ TeV and $\sqrt{s} = 7$ TeV, *Phys. Lett. B* 717 (2012) 162, arXiv:1205.5724 [hep-ex].
- [63] L. Altenkämper, F. Bock, C. Loizides, N. Schmidt, Applicability of transverse mass scaling in hadronic collisions at energies available at the CERN Large Hadron Collider, *Phys. Rev. C* 96 (2017) 064907, arXiv:1710.01933 [hep-ph].
- [64] ALICE Collaboration, B. Abelev, et al., Production of $K^*(892)^0$ and $\phi(1020)$ in pp collisions at $\sqrt{s} = 7$ TeV, *Eur. Phys. J. C* 72 (2012) 2183, arXiv:1208.5717 [hep-ex].
- [65] P.Z. Skands, Tuning Monte Carlo generators: The Perugia tunes, *Phys. Rev. D* 82 (2010) 074018, arXiv:1005.3457 [hep-ph].
- [66] P. Nason, A new method for combining NLO QCD with shower Monte Carlo algorithms, *J. High Energy Phys.* 11 (2004) 040, arXiv:hep-ph/0409146 [hep-ph].
- [67] S. Frixione, P. Nason, G. Ridolfi, A positive-weight next-to-leading-order Monte Carlo for heavy flavour hadroproduction, *J. High Energy Phys.* 09 (2007) 126, arXiv:0707.3088 [hep-ph].
- [68] S. Frixione, P. Nason, C. Oleari, Matching NLO QCD computations with parton shower simulations: the POWHEG method, *J. High Energy Phys.* 11 (2007) 070, arXiv:0709.2092 [hep-ph].
- [69] S. Alioli, P. Nason, C. Oleari, E. Re, A general framework for implementing NLO calculations in shower Monte Carlo programs: the POWHEG BOX, *J. High Energy Phys.* 06 (2010) 043, arXiv:1002.2581 [hep-ph].
- [70] R. Averbeck, N. Bastid, Z.C. del Valle, P. Crochet, A. Dainese, X. Zhang, Reference heavy flavour cross sections in pp collisions at $\sqrt{s} = 2.76$ TeV, using a pQCD-driven \sqrt{s} -scaling of ALICE measurements at $\sqrt{s} = 7$ TeV, arXiv:1107.3243 [hep-ph].
- [71] M. Cacciari, M.L. Mangano, P. Nason, Gluon PDF constraints from the ratio of forward heavy-quark production at the LHC at $\sqrt{s} = 7$ and 13 TeV, *Eur. Phys. J. C* 75 (2015) 610, arXiv:1507.06197 [hep-ph].
- [72] ALICE Collaboration, K. Aamodt, et al., Rapidity and transverse momentum dependence of inclusive J/ψ production in pp collisions at $\sqrt{s} = 7$ TeV, *Phys. Lett. B* 704 (2011) 442, arXiv:1105.0380 [hep-ex], Erratum: *Phys. Lett. B* 718 (2012) 692.
- [73] ALICE Collaboration, J. Adam, et al., Inclusive quarkonium production at forward rapidity in pp collisions at $\sqrt{s} = 8$ TeV, *Eur. Phys. J. C* 76 (2016) 184, arXiv:1509.08258 [hep-ex].
- [74] Particle Data Group, C. Patrignani, et al., Review of Particle Physics, *Chin. Phys. C* 40 (2016) 100001.
- [75] ALICE Collaboration, S. Acharya, et al., Λ_c^+ production in pp collisions at $\sqrt{s} = 7$ TeV and in p–Pb collisions at $\sqrt{s_{NN}} = 5.02$ TeV, *J. High Energy Phys.* 1804 (2018) 108, [https://doi.org/10.1007/JHEP04\(2018\)108](https://doi.org/10.1007/JHEP04(2018)108), arXiv:1712.09581 [nucl-ex].
- [76] L. Gladilin, Fragmentation fractions of c and b quarks into charmed hadrons at LEP, *Eur. Phys. J. C* 75 (2015), arXiv:1404.3888 [hep-ex].
- [77] N.M. Kroll, W. Wada, Internal pair production associated with the emission of high-energy gamma rays, *Phys. Rev.* 98 (1955) 1355.
- [78] L.G. Landsberg, Electromagnetic decays of light mesons, *Phys. Rep.* 128 (1985) 301.
- [79] G.J. Feldman, R.D. Cousins, Unified approach to the classical statistical analysis of small signals, *Phys. Rev. D* 57 (1998) 3873, arXiv:physics/9711021 [physics.data-an].
- [80] L.E. Gordon, W. Vogelsang, Polarized and unpolarized prompt photon production beyond the leading order, *Phys. Rev. D* 48 (1993) 3136.

ALICE Collaboration

S. Acharya¹³⁹, F. Torales-Acosta²⁰, D. Adamová⁹³, J. Adolfsson⁸⁰, M.M. Aggarwal⁹⁸, G. Aglieri Rinella³⁴, M. Agnello³¹, N. Agrawal⁴⁸, Z. Ahammed¹³⁹, S.U. Ahn⁷⁶, S. Aiola¹⁴⁴, A. Akindinov⁶⁴, M. Al-Turany¹⁰⁴, S.N. Alam¹³⁹, D.S.D. Albuquerque¹²¹, D. Aleksandrov⁸⁷, B. Alessandro⁵⁸, R. Alfaro Molina⁷², Y. Ali¹⁵, A. Alici^{10,27,53}, A. Alkin², J. Alme²², T. Alt⁶⁹, L. Altenkamper²², I. Altsybeev¹¹¹, M.N. Anaam⁶, C. Andrei⁴⁷, D. Andreou³⁴, H.A. Andrews¹⁰⁸, A. Andronic^{142,104}, M. Angeletti³⁴, V. Anguelov¹⁰², C. Anson¹⁶, T. Antičić¹⁰⁵, F. Antinori⁵⁶, P. Antonioli⁵³, R. Anwar¹²⁵, N. Apadula⁷⁹, L. Aphecetche¹¹³, H. Appelshäuser⁶⁹, S. Arcelli²⁷, R. Arnaldi⁵⁸, O.W. Arnold^{103,116}, I.C. Arsene²¹, M. Arslanok¹⁰², A. Augustinus³⁴, R. Averbeck¹⁰⁴, M.D. Azmi¹⁷, A. Badalà⁵⁵, Y.W. Baek^{60,40}, S. Bagnasco⁵⁸, R. Bailhache⁶⁹, R. Bala⁹⁹, A. Baldissari¹³⁵, M. Ball⁴², R.C. Baral⁸⁵, A.M. Barbano²⁶, R. Barbera²⁸, F. Barile⁵², L. Barioglio²⁶, G.G. Barnaföldi¹⁴³, L.S. Barnby⁹², V. Barret¹³², P. Bartalini⁶, K. Barth³⁴, E. Bartsch⁶⁹, N. Bastid¹³², S. Basu¹⁴¹, G. Batigne¹¹³, B. Batyunya⁷⁵, P.C. Batzing²¹, J.L. Bazo Alba¹⁰⁹, I.G. Bearden⁸⁸, H. Beck¹⁰², C. Bedda⁶³, N.K. Behera⁶⁰, I. Belikov¹³⁴, F. Bellini³⁴, H. Bello Martinez⁴⁴, R. Bellwied¹²⁵, L.G.E. Beltran¹¹⁹, V. Belyaev⁹¹, G. Bencedi¹⁴³, S. Beole²⁶, A. Bercuci⁴⁷, Y. Berdnikov⁹⁶, D. Berenyi¹⁴³, R.A. Bertens¹²⁸, D. Berzana^{34,58}, L. Betev³⁴, P.P. Bhaduri¹³⁹, A. Bhasin⁹⁹, I.R. Bhat⁹⁹, H. Bhatt⁴⁸, B. Bhattacharjee⁴¹, J. Bhom¹¹⁷, A. Bianchi²⁶, L. Bianchi¹²⁵, N. Bianchi⁵¹, J. Bielčík³⁷, J. Bielčíková⁹³, A. Bilandžić^{116,103}, G. Biro¹⁴³, R. Biswas³, S. Biswas³, J.T. Blair¹¹⁸, D. Blau⁸⁷, C. Blume⁶⁹, G. Boca¹³⁷, F. Bock³⁴, A. Bogdanov⁹¹, L. Boldizsár¹⁴³, M. Bombara³⁸, G. Bonomi¹³⁸, M. Bonora³⁴, H. Borel¹³⁵, A. Borissov¹⁴², M. Borri¹²⁷, E. Botta²⁶, C. Bourjau⁸⁸, L. Bratrud⁶⁹,

- P. Braun-Munzinger ¹⁰⁴, M. Bregant ¹²⁰, T.A. Broker ⁶⁹, M. Broz ³⁷, E.J. Brucken ⁴³, E. Bruna ⁵⁸,
 G.E. Bruno ^{34,33}, D. Budnikov ¹⁰⁶, H. Buesching ⁶⁹, S. Bufalino ³¹, P. Buhler ¹¹², P. Buncic ³⁴, O. Busch ^{131,i},
 Z. Buthelezi ⁷³, J.B. Butt ¹⁵, J.T. Buxton ⁹⁵, J. Cabala ¹¹⁵, D. Caffarri ⁸⁹, H. Caines ¹⁴⁴, A. Caliva ¹⁰⁴,
 E. Calvo Villar ¹⁰⁹, R.S. Camacho ⁴⁴, P. Camerini ²⁵, A.A. Capon ¹¹², F. Carena ³⁴, W. Carena ³⁴,
 F. Carnesecchi ^{27,10}, J. Castillo Castellanos ¹³⁵, A.J. Castro ¹²⁸, E.A.R. Casula ⁵⁴, C. Ceballos Sanchez ⁸,
 S. Chandra ¹³⁹, B. Chang ¹²⁶, W. Chang ⁶, S. Chapelard ³⁴, M. Chartier ¹²⁷, S. Chattopadhyay ¹³⁹,
 S. Chattopadhyay ¹⁰⁷, A. Chauvin ^{103,116}, C. Cheshkov ¹³³, B. Cheynis ¹³³, V. Chibante Barroso ³⁴,
 D.D. Chinellato ¹²¹, S. Cho ⁶⁰, P. Chochula ³⁴, T. Chowdhury ¹³², P. Christakoglou ⁸⁹, C.H. Christensen ⁸⁸,
 P. Christiansen ⁸⁰, T. Chujo ¹³¹, S.U. Chung ¹⁸, C. Cicalo ⁵⁴, L. Cifarelli ^{10,27}, F. Cindolo ⁵³, J. Cleymans ¹²⁴,
 F. Colamaria ⁵², D. Colella ^{65,52}, A. Collu ⁷⁹, M. Colocci ²⁷, M. Concas ^{58,ii}, G. Conesa Balbastre ⁷⁸,
 Z. Conesa del Valle ⁶¹, J.G. Contreras ³⁷, T.M. Cormier ⁹⁴, Y. Corrales Morales ⁵⁸, P. Cortese ³²,
 M.R. Cosentino ¹²², F. Costa ³⁴, S. Costanza ¹³⁷, J. Crkovská ⁶¹, P. Crochet ¹³², E. Cuautle ⁷⁰,
 L. Cunqueiro ^{142,94}, T. Dahms ^{103,116}, A. Dainese ⁵⁶, S. Dani ⁶⁶, M.C. Danisch ¹⁰², A. Danu ⁶⁸, D. Das ¹⁰⁷,
 I. Das ¹⁰⁷, S. Das ³, A. Dash ⁸⁵, S. Dash ⁴⁸, A. Dashi ^{103,116}, S. De ⁴⁹, A. De Caro ³⁰, G. de Cataldo ⁵²,
 C. de Conti ¹²⁰, J. de Cuveland ³⁹, A. De Falco ²⁴, D. De Gruttola ^{10,30}, N. De Marco ⁵⁸, S. De Pasquale ³⁰,
 R.D. De Souza ¹²¹, H.F. Degenhardt ¹²⁰, A. Deisting ^{104,102}, A. Deloff ⁸⁴, S. Delsanto ²⁶, C. Deplano ⁸⁹,
 P. Dhankher ⁴⁸, D. Di Bari ³³, A. Di Mauro ³⁴, B. Di Ruzza ⁵⁶, R.A. Diaz ⁸, T. Dietel ¹²⁴, P. Dillenseger ⁶⁹,
 Y. Ding ⁶, R. Divià ³⁴, Ø. Djupsland ²², A. Dobrin ³⁴, D. Domenicis Gimenez ¹²⁰, B. Dönigus ⁶⁹, O. Dordic ²¹,
 L.V.R. Doremalen ⁶³, A.K. Dubey ¹³⁹, A. Dubla ¹⁰⁴, L. Ducroux ¹³³, S. Dudi ⁹⁸, A.K. Duggal ⁹⁸,
 M. Dukhishyam ⁸⁵, P. Dupieux ¹³², R.J. Ehlers ¹⁴⁴, D. Elia ⁵², E. Endress ¹⁰⁹, H. Engel ⁷⁴, E. Epple ¹⁴⁴,
 B. Erazmus ¹¹³, F. Erhardt ⁹⁷, M.R. Ersdal ²², B. Espagnon ⁶¹, G. Eulisse ³⁴, J. Eum ¹⁸, D. Evans ¹⁰⁸,
 S. Evdokimov ⁹⁰, L. Fabbietti ^{103,116}, M. Faggin ²⁹, J. Faivre ⁷⁸, A. Fantoni ⁵¹, M. Fasel ⁹⁴, L. Feldkamp ¹⁴²,
 A. Feliciello ⁵⁸, G. Feofilov ¹¹¹, A. Fernández Téllez ⁴⁴, A. Ferretti ²⁶, A. Festanti ³⁴, V.J.G. Feuillard ¹⁰²,
 J. Figiel ¹¹⁷, M.A.S. Figueiredo ¹²⁰, S. Filchagin ¹⁰⁶, D. Finogeev ⁶², F.M. Fionda ²², G. Fiorenza ⁵², F. Flor ¹²⁵,
 M. Floris ³⁴, S. Foertsch ⁷³, P. Foka ¹⁰⁴, S. Fokin ⁸⁷, E. Fragiocomo ⁵⁹, A. Francescon ³⁴, A. Francisco ¹¹³,
 U. Frankenfeld ¹⁰⁴, G.G. Fronze ²⁶, U. Fuchs ³⁴, C. Furget ⁷⁸, A. Furs ⁶², M. Fusco Girard ³⁰, J.J. Gaardhøje ⁸⁸,
 M. Gagliardi ²⁶, A.M. Gago ¹⁰⁹, K. Gajdosova ⁸⁸, M. Gallio ²⁶, C.D. Galvan ¹¹⁹, P. Ganoti ⁸³, C. Garabatos ¹⁰⁴,
 E. Garcia-Solis ¹¹, K. Garg ²⁸, C. Gargiulo ³⁴, P. Gasik ^{116,103}, E.F. Gauger ¹¹⁸, M.B. Gay Ducati ⁷¹,
 M. Germain ¹¹³, J. Ghosh ¹⁰⁷, P. Ghosh ¹³⁹, S.K. Ghosh ³, P. Gianotti ⁵¹, P. Giubellino ^{104,58}, P. Giubilato ²⁹,
 P. Glässel ¹⁰², D.M. Goméz Coral ⁷², A. Gomez Ramirez ⁷⁴, V. Gonzalez ¹⁰⁴, P. González-Zamora ⁴⁴,
 S. Gorbunov ³⁹, L. Görlich ¹¹⁷, S. Gotovac ³⁵, V. Grabski ⁷², L.K. Graczykowski ¹⁴⁰, K.L. Graham ¹⁰⁸,
 L. Greiner ⁷⁹, A. Grelli ⁶³, C. Grigoras ³⁴, V. Grigoriev ⁹¹, A. Grigoryan ¹, S. Grigoryan ⁷⁵, J.M. Gronefeld ¹⁰⁴,
 F. Grossa ³¹, J.F. Grosse-Oetringhaus ³⁴, R. Grossos ¹⁰⁴, R. Guernane ⁷⁸, B. Guerzoni ²⁷, M. Guittiere ¹¹³,
 K. Gulbrandsen ⁸⁸, T. Gunji ¹³⁰, A. Gupta ⁹⁹, R. Gupta ⁹⁹, I.B. Guzman ⁴⁴, R. Haake ³⁴, M.K. Habib ¹⁰⁴,
 C. Hadjidakis ⁶¹, H. Hamagaki ⁸¹, G. Hamar ¹⁴³, M. Hamid ⁶, J.C. Hamon ¹³⁴, R. Hannigan ¹¹⁸,
 M.R. Haque ⁶³, A. Harlenderova ¹⁰⁴, J.W. Harris ¹⁴⁴, A. Harton ¹¹, H. Hassan ⁷⁸, D. Hatzifotiadou ^{53,10},
 S. Hayashi ¹³⁰, S.T. Heckel ⁶⁹, E. Hellbär ⁶⁹, H. Helstrup ³⁶, A. Herghelegiu ⁴⁷, E.G. Hernandez ⁴⁴,
 G. Herrera Corral ⁹, F. Herrmann ¹⁴², K.F. Hetland ³⁶, T.E. Hilden ⁴³, H. Hillemanns ³⁴, C. Hills ¹²⁷,
 B. Hippolyte ¹³⁴, B. Hohlweyer ¹⁰³, D. Horak ³⁷, S. Hornung ¹⁰⁴, R. Hosokawa ^{131,78}, J. Hota ⁶⁶, P. Hristov ³⁴,
 C. Huang ⁶¹, C. Hughes ¹²⁸, P. Huhn ⁶⁹, T.J. Humanic ⁹⁵, H. Hushnud ¹⁰⁷, N. Hussain ⁴¹, T. Hussain ¹⁷,
 D. Hutter ³⁹, D.S. Hwang ¹⁹, J.P. Iddon ¹²⁷, S.A. Iga Buitron ⁷⁰, R. Illkaev ¹⁰⁶, M. Inaba ¹³¹, M. Ippolitov ⁸⁷,
 M.S. Islam ¹⁰⁷, M. Ivanov ¹⁰⁴, V. Ivanov ⁹⁶, V. Izucheev ⁹⁰, B. Jacak ⁷⁹, N. Jacazio ²⁷, P.M. Jacobs ⁷⁹,
 M.B. Jadhav ⁴⁸, S. Jadlovska ¹¹⁵, J. Jadlovsky ¹¹⁵, S. Jaelani ⁶³, C. Jahnke ^{120,116}, M.J. Jakubowska ¹⁴⁰,
 M.A. Janik ¹⁴⁰, C. Jena ⁸⁵, M. Jercic ⁹⁷, O. Jevons ¹⁰⁸, R.T. Jimenez Bustamante ¹⁰⁴, M. Jin ¹²⁵, P.G. Jones ¹⁰⁸,
 A. Jusko ¹⁰⁸, P. Kalinak ⁶⁵, A. Kalweit ³⁴, J.H. Kang ¹⁴⁵, V. Kaplin ⁹¹, S. Kar ⁶, A. Karasu Uysal ⁷⁷,
 O. Karavichev ⁶², T. Karavicheva ⁶², P. Karczmarczyk ³⁴, E. Karpechev ⁶², U. Kebschull ⁷⁴, R. Keidel ⁴⁶,
 D.L.D. Keijdener ⁶³, M. Keil ³⁴, B. Ketzer ⁴², Z. Khabanova ⁸⁹, A.M. Khan ⁶, S. Khan ¹⁷, S.A. Khan ¹³⁹,
 A. Khanzadeev ⁹⁶, Y. Kharlov ⁹⁰, A. Khatun ¹⁷, A. Khuntia ⁴⁹, M.M. Kielbowicz ¹¹⁷, B. Kileng ³⁶, B. Kim ¹³¹,
 D. Kim ¹⁴⁵, D.J. Kim ¹²⁶, E.J. Kim ¹³, H. Kim ¹⁴⁵, J.S. Kim ⁴⁰, J. Kim ¹⁰², M. Kim ^{60,102}, S. Kim ¹⁹, T. Kim ¹⁴⁵,
 T. Kim ¹⁴⁵, S. Kirsch ³⁹, I. Kisel ³⁹, S. Kiselev ⁶⁴, A. Kisiel ¹⁴⁰, J.L. Klay ⁵, C. Klein ⁶⁹, J. Klein ^{34,58},
 C. Klein-Bösing ¹⁴², S. Klewin ¹⁰², A. Kluge ³⁴, M.L. Knichel ³⁴, A.G. Knospe ¹²⁵, C. Kobdaj ¹¹⁴,
 M. Kofarago ¹⁴³, M.K. Köhler ¹⁰², T. Kollegger ¹⁰⁴, N. Kondratyeva ⁹¹, E. Kondratyuk ⁹⁰, A. Konevskikh ⁶²,

- P.J. Konopka ³⁴, M. Konyushikhin ¹⁴¹, O. Kovalenko ⁸⁴, V. Kovalenko ¹¹¹, M. Kowalski ¹¹⁷, I. Králík ⁶⁵, A. Kravčáková ³⁸, L. Kreis ¹⁰⁴, M. Krivda ^{65,108}, F. Krizek ⁹³, M. Krüger ⁶⁹, E. Kryshen ⁹⁶, M. Krzewicki ³⁹, A.M. Kubera ⁹⁵, V. Kučera ^{93,60}, C. Kuhn ¹³⁴, P.G. Kuijer ⁸⁹, J. Kumar ⁴⁸, L. Kumar ⁹⁸, S. Kumar ⁴⁸, S. Kundu ⁸⁵, P. Kurashvili ⁸⁴, A. Kurepin ⁶², A.B. Kurepin ⁶², A. Kuryakin ¹⁰⁶, S. Kushpil ⁹³, J. Kvapil ¹⁰⁸, M.J. Kweon ⁶⁰, Y. Kwon ¹⁴⁵, S.L. La Pointe ³⁹, P. La Rocca ²⁸, Y.S. Lai ⁷⁹, I. Lakomov ³⁴, R. Langoy ¹²³, K. Lapidus ¹⁴⁴, A. Lardeux ²¹, P. Larionov ⁵¹, E. Laudi ³⁴, R. Lavicka ³⁷, R. Lea ²⁵, L. Leardini ¹⁰², S. Lee ¹⁴⁵, F. Lehas ⁸⁹, S. Lehner ¹¹², J. Lehrbach ³⁹, R.C. Lemmon ⁹², I. León Monzón ¹¹⁹, P. Lévai ¹⁴³, X. Li ¹², X.L. Li ⁶, J. Lien ¹²³, R. Lietava ¹⁰⁸, B. Lim ¹⁸, S. Lindal ²¹, V. Lindenstruth ³⁹, S.W. Lindsay ¹²⁷, C. Lippmann ¹⁰⁴, M.A. Lisa ⁹⁵, V. Litichevskyi ⁴³, A. Liu ⁷⁹, H.M. Ljunggren ⁸⁰, W.J. Llope ¹⁴¹, D.F. Lodato ⁶³, V. Loginov ⁹¹, C. Loizides ^{94,79}, P. Loncar ³⁵, X. Lopez ¹³², E. López Torres ⁸, A. Lowe ¹⁴³, P. Luettig ⁶⁹, J.R. Luhder ¹⁴², M. Lunardon ²⁹, G. Luparello ⁵⁹, M. Lupi ³⁴, A. Maevskaia ⁶², M. Mager ³⁴, S.M. Mahmood ²¹, A. Maire ¹³⁴, R.D. Majka ¹⁴⁴, M. Malaev ⁹⁶, Q.W. Malik ²¹, L. Malinina ^{75,iii}, D. Mal'Kevich ⁶⁴, P. Malzacher ¹⁰⁴, A. Mamontov ¹⁰⁶, V. Manko ⁸⁷, F. Manso ¹³², V. Manzari ⁵², Y. Mao ⁶, M. Marchisone ^{129,73,133}, J. Mareš ⁶⁷, G.V. Margagliotti ²⁵, A. Margotti ⁵³, J. Margutti ⁶³, A. Marín ¹⁰⁴, C. Markert ¹¹⁸, M. Marquard ⁶⁹, N.A. Martin ¹⁰⁴, P. Martinengo ³⁴, J.L. Martinez ¹²⁵, M.I. Martínez ⁴⁴, G. Martínez García ¹¹³, M. Martinez Pedreira ³⁴, S. Masciocchi ¹⁰⁴, M. Masera ²⁶, A. Masoni ⁵⁴, L. Massacrier ⁶¹, E. Masson ¹¹³, A. Mastroserio ^{52,136}, A.M. Mathis ^{116,103}, P.F.T. Matuoka ¹²⁰, A. Matyja ^{117,128}, C. Mayer ¹¹⁷, M. Mazzilli ³³, M.A. Mazzoni ⁵⁷, F. Meddi ²³, Y. Melikyan ⁹¹, A. Menchaca-Rocha ⁷², E. Meninno ³⁰, J. Mercado Pérez ¹⁰², M. Meres ¹⁴, C.S. Meza ¹⁰⁹, S. Mhlanga ¹²⁴, Y. Miake ¹³¹, L. Micheletti ²⁶, M.M. Mieskolainen ⁴³, D.L. Mihaylov ¹⁰³, K. Mikhaylov ^{64,75}, A. Mischke ⁶³, A.N. Mishra ⁷⁰, D. Miśkowiec ¹⁰⁴, J. Mitra ¹³⁹, C.M. Mitu ⁶⁸, N. Mohammadi ³⁴, A.P. Mohanty ⁶³, B. Mohanty ⁸⁵, M. Mohisin Khan ^{17,iv}, D.A. Moreira De Godoy ¹⁴², L.A.P. Moreno ⁴⁴, S. Moretto ²⁹, A. Morreale ¹¹³, A. Morsch ³⁴, T. Mrnjavac ³⁴, V. Muccifora ⁵¹, E. Mudnic ³⁵, D. Mühlheim ¹⁴², S. Muhuri ¹³⁹, M. Mukherjee ³, J.D. Mulligan ¹⁴⁴, M.G. Munhoz ¹²⁰, K. Münning ⁴², M.I.A. Munoz ⁷⁹, R.H. Munzer ⁶⁹, H. Murakami ¹³⁰, S. Murray ⁷³, L. Musa ³⁴, J. Musinsky ⁶⁵, C.J. Myers ¹²⁵, J.W. Myrcha ¹⁴⁰, B. Naik ⁴⁸, R. Nair ⁸⁴, B.K. Nandi ⁴⁸, R. Nania ^{53,10}, E. Nappi ⁵², A. Narayan ⁴⁸, M.U. Naru ¹⁵, A.F. Nassirpour ⁸⁰, H. Natal da Luz ¹²⁰, C. Natrass ¹²⁸, S.R. Navarro ⁴⁴, K. Nayak ⁸⁵, R. Nayak ⁴⁸, T.K. Nayak ¹³⁹, S. Nazarenko ¹⁰⁶, R.A. Negrao De Oliveira ^{69,34}, L. Nellen ⁷⁰, S.V. Nesbo ³⁶, G. Neskovic ³⁹, F. Ng ¹²⁵, M. Nicassio ¹⁰⁴, J. Niedziela ^{140,34}, B.S. Nielsen ⁸⁸, S. Nikolaev ⁸⁷, S. Nikulin ⁸⁷, V. Nikulin ⁹⁶, F. Noferini ^{10,53}, P. Nomokonov ⁷⁵, G. Nooren ⁶³, J.C.C. Noris ⁴⁴, J. Norman ⁷⁸, A. Nyanin ⁸⁷, J. Nystrand ²², H. Oh ¹⁴⁵, A. Ohlson ¹⁰², J. Oleniacz ¹⁴⁰, A.C. Oliveira Da Silva ¹²⁰, M.H. Oliver ¹⁴⁴, J. Onderwaater ¹⁰⁴, C. Oppedisano ⁵⁸, R. Orava ⁴³, M. Oravec ¹¹⁵, A. Ortiz Velasquez ⁷⁰, A. Oskarsson ⁸⁰, J. Otwinowski ¹¹⁷, K. Oyama ⁸¹, Y. Pachmayer ¹⁰², V. Pacik ⁸⁸, D. Pagano ¹³⁸, G. Paić ⁷⁰, P. Palni ⁶, J. Pan ¹⁴¹, A.K. Pandey ⁴⁸, S. Panebianco ¹³⁵, V. Papikyan ¹, P. Pareek ⁴⁹, J. Park ⁶⁰, J.E. Parkkila ¹²⁶, S. Parmar ⁹⁸, A. Passfeld ¹⁴², S.P. Pathak ¹²⁵, R.N. Patra ¹³⁹, B. Paul ⁵⁸, H. Pei ⁶, T. Peitzmann ⁶³, X. Peng ⁶, L.G. Pereira ⁷¹, H. Pereira Da Costa ¹³⁵, D. Peresunko ⁸⁷, E. Perez Lezama ⁶⁹, V. Peskov ⁶⁹, Y. Pestov ⁴, V. Petráček ³⁷, M. Petrovici ⁴⁷, C. Petta ²⁸, R.P. Pezzi ⁷¹, S. Piano ⁵⁹, M. Pikna ¹⁴, P. Pillot ¹¹³, L.O.D.L. Pimentel ⁸⁸, O. Pinazza ^{53,34}, L. Pinsky ¹²⁵, S. Pisano ⁵¹, D.B. Piyarathna ¹²⁵, M. Płoskoń ⁷⁹, M. Planinic ⁹⁷, F. Pliquet ⁶⁹, J. Pluta ¹⁴⁰, S. Pochybova ¹⁴³, P.L.M. Podesta-Lerma ¹¹⁹, M.G. Poghosyan ⁹⁴, B. Polichtchouk ⁹⁰, N. Poljak ⁹⁷, W. Poonsawat ¹¹⁴, A. Pop ⁴⁷, H. Poppenborg ¹⁴², S. Porteboeuf-Houssais ¹³², V. Pozdniakov ⁷⁵, S.K. Prasad ³, R. Preghenella ⁵³, F. Prino ⁵⁸, C.A. Pruneau ¹⁴¹, I. Pshenichnov ⁶², M. Puccio ²⁶, V. Punin ¹⁰⁶, J. Putschke ¹⁴¹, S. Raha ³, S. Rajput ⁹⁹, J. Rak ¹²⁶, A. Rakotozafindrabe ¹³⁵, L. Ramello ³², F. Rami ¹³⁴, R. Raniwala ¹⁰⁰, S. Raniwala ¹⁰⁰, S.S. Räsänen ⁴³, B.T. Rascanu ⁶⁹, V. Ratza ⁴², I. Ravasenga ³¹, K.F. Read ^{128,94}, K. Redlich ^{84,v}, A. Rehman ²², P. Reichelt ⁶⁹, F. Reidt ³⁴, X. Ren ⁶, R. Renfordt ⁶⁹, A. Reshetin ⁶², J.-P. Revol ¹⁰, K. Reygers ¹⁰², V. Riabov ⁹⁶, T. Richert ⁶³, M. Richter ²¹, P. Riedler ³⁴, W. Riegler ³⁴, F. Riggii ²⁸, C. Ristea ⁶⁸, S.P. Rode ⁴⁹, M. Rodríguez Cahuantzi ⁴⁴, K. Røed ²¹, R. Rogalev ⁹⁰, E. Rogochaya ⁷⁵, D. Rohr ³⁴, D. Röhrich ²², P.S. Rokita ¹⁴⁰, F. Ronchetti ⁵¹, E.D. Rosas ⁷⁰, K. Roslon ¹⁴⁰, P. Rosnet ¹³², A. Rossi ²⁹, A. Rotondi ¹³⁷, F. Roukoutakis ⁸³, C. Roy ¹³⁴, P. Roy ¹⁰⁷, O.V. Rueda ⁷⁰, R. Rui ²⁵, B. Rumyantsev ⁷⁵, A. Rustamov ⁸⁶, E. Ryabinkin ⁸⁷, Y. Ryabov ⁹⁶, A. Rybicki ¹¹⁷, S. Saarinen ⁴³, S. Sadhu ¹³⁹, S. Sadovsky ⁹⁰, K. Šafařík ³⁴, S.K. Saha ¹³⁹, B. Sahoo ⁴⁸, P. Sahoo ⁴⁹, R. Sahoo ⁴⁹, S. Sahoo ⁶⁶, P.K. Sahu ⁶⁶, J. Saini ¹³⁹, S. Sakai ¹³¹, M.A. Saleh ¹⁴¹, S. Sambyal ⁹⁹, V. Samsonov ^{96,91}, A. Sandoval ⁷², A. Sarkar ⁷³, D. Sarkar ¹³⁹, N. Sarkar ¹³⁹, P. Sarma ⁴¹, M.H.P. Sas ⁶³, E. Scapparone ⁵³, F. Scarlassara ²⁹, B. Schaefer ⁹⁴,

- H.S. Scheid ⁶⁹, C. Schiaua ⁴⁷, R. Schicker ¹⁰², C. Schmidt ¹⁰⁴, H.R. Schmidt ¹⁰¹, M.O. Schmidt ¹⁰²,
 M. Schmidt ¹⁰¹, N.V. Schmidt ^{94,69}, J. Schukraft ³⁴, Y. Schutz ^{34,134}, K. Schwarz ¹⁰⁴, K. Schweda ¹⁰⁴,
 G. Scioli ²⁷, E. Scomparin ⁵⁸, M. Šefčík ³⁸, J.E. Seger ¹⁶, Y. Sekiguchi ¹³⁰, D. Sekihata ⁴⁵,
 I. Selyuzhenkov ^{104,91}, S. Senyukov ¹³⁴, E. Serradilla ⁷², P. Sett ⁴⁸, A. Sevcenco ⁶⁸, A. Shabanov ⁶²,
 A. Shabetai ¹¹³, R. Shahoyan ³⁴, W. Shaikh ¹⁰⁷, A. Shangaraev ⁹⁰, A. Sharma ⁹⁸, A. Sharma ⁹⁹, M. Sharma ⁹⁹,
 N. Sharma ⁹⁸, A.I. Sheikh ¹³⁹, K. Shigaki ⁴⁵, M. Shimomura ⁸², S. Shirinkin ⁶⁴, Q. Shou ^{6,110}, K. Shtejer ²⁶,
 Y. Sibiriak ⁸⁷, S. Siddhanta ⁵⁴, K.M. Sielewicz ³⁴, T. Siemianczuk ⁸⁴, D. Silvermyr ⁸⁰, G. Simatovic ⁸⁹,
 G. Simonetti ^{34,103}, R. Singaraju ¹³⁹, R. Singh ⁸⁵, R. Singh ⁹⁹, V. Singhal ¹³⁹, T. Sinha ¹⁰⁷, B. Sitar ¹⁴,
 M. Sitta ³², T.B. Skaali ²¹, M. Slupecki ¹²⁶, N. Smirnov ¹⁴⁴, R.J.M. Snellings ⁶³, T.W. Snellman ¹²⁶, J. Song ¹⁸,
 F. Soramel ²⁹, S. Sorensen ¹²⁸, F. Sozzi ¹⁰⁴, I. Sputowska ¹¹⁷, J. Stachel ¹⁰², I. Stan ⁶⁸, P. Stankus ⁹⁴,
 E. Stenlund ⁸⁰, D. Stocco ¹¹³, M.M. Storetvedt ³⁶, P. Strmen ¹⁴, A.A.P. Suade ¹²⁰, T. Sugitate ⁴⁵, C. Suire ⁶¹,
 M. Suleymanov ¹⁵, M. Suljic ^{34,25}, R. Sultanov ⁶⁴, M. Šumbera ⁹³, S. Sumowidagdo ⁵⁰, K. Suzuki ¹¹²,
 S. Swain ⁶⁶, A. Szabo ¹⁴, I. Szarka ¹⁴, U. Tabassam ¹⁵, J. Takahashi ¹²¹, G.J. Tambave ²², N. Tanaka ¹³¹,
 M. Tarhini ¹¹³, M. Tariq ¹⁷, M.G. Tarzila ⁴⁷, A. Tauro ³⁴, G. Tejeda Muñoz ⁴⁴, A. Telesca ³⁴, C. Terrevoli ²⁹,
 B. Teyssier ¹³³, D. Thakur ⁴⁹, S. Thakur ¹³⁹, D. Thomas ¹¹⁸, F. Thoresen ⁸⁸, R. Tieulent ¹³³, A. Tikhonov ⁶²,
 A.R. Timmins ¹²⁵, A. Toia ⁶⁹, N. Topilskaya ⁶², M. Toppi ⁵¹, S.R. Torres ¹¹⁹, S. Tripathy ⁴⁹, S. Trogolo ²⁶,
 G. Trombetta ³³, L. Tropp ³⁸, V. Trubnikov ², W.H. Trzaska ¹²⁶, T.P. Trzcinski ¹⁴⁰, B.A. Trzeciak ⁶³,
 T. Tsuji ¹³⁰, A. Tumkin ¹⁰⁶, R. Turrisi ⁵⁶, T.S. Tveter ²¹, K. Ullaland ²², E.N. Umaka ¹²⁵, A. Uras ¹³³,
 G.L. Usai ²⁴, A. Utrobiticic ⁹⁷, M. Vala ¹¹⁵, J.W. Van Hoorn ³⁴, M. van Leeuwen ⁶³, P. Vande Vyvre ³⁴,
 D. Varga ¹⁴³, A. Vargas ⁴⁴, M. Vargyas ¹²⁶, R. Varma ⁴⁸, M. Vasileiou ⁸³, A. Vasiliev ⁸⁷, A. Vauthier ⁷⁸,
 O. Vázquez Doce ^{103,116}, V. Vechernin ¹¹¹, A.M. Veen ⁶³, E. Vercellin ²⁶, S. Vergara Limón ⁴⁴, L. Vermunt ⁶³,
 R. Vernet ⁷, R. Vértesi ¹⁴³, L. Vickovic ³⁵, J. Viinikainen ¹²⁶, Z. Vilakazi ¹²⁹, O. Villalobos Baillie ¹⁰⁸,
 A. Villatoro Tello ⁴⁴, A. Vinogradov ⁸⁷, T. Virgili ³⁰, V. Vislavicius ^{88,80}, A. Vodopyanov ⁷⁵, M.A. Völkl ¹⁰¹,
 K. Voloshin ⁶⁴, S.A. Voloshin ¹⁴¹, G. Volpe ³³, B. von Haller ³⁴, I. Vorobyev ^{116,103}, D. Voscek ¹¹⁵,
 D. Vranic ^{104,34}, J. Vrláková ³⁸, B. Wagner ²², H. Wang ⁶³, M. Wang ⁶, Y. Watanabe ¹³¹, M. Weber ¹¹²,
 S.G. Weber ¹⁰⁴, A. Wegrzynek ³⁴, D.F. Weiser ¹⁰², S.C. Wenzel ³⁴, J.P. Wessels ¹⁴², U. Westerhoff ¹⁴²,
 A.M. Whitehead ¹²⁴, J. Wiechula ⁶⁹, J. Wikne ²¹, G. Wilk ⁸⁴, J. Wilkinson ⁵³, G.A. Willem ^{142,34},
 M.C.S. Williams ⁵³, E. Willsher ¹⁰⁸, B. Windelband ¹⁰², W.E. Witt ¹²⁸, R. Xu ⁶, S. Yalcin ⁷⁷, K. Yamakawa ⁴⁵,
 S. Yano ⁴⁵, Z. Yin ⁶, H. Yokoyama ^{78,131}, I.-K. Yoo ¹⁸, J.H. Yoon ⁶⁰, V. Yurchenko ², V. Zaccolo ⁵⁸,
 A. Zaman ¹⁵, C. Zampolli ³⁴, H.J.C. Zanolli ¹²⁰, N. Zardoshti ¹⁰⁸, A. Zarochentsev ¹¹¹, P. Závada ⁶⁷,
 N. Zaviyalov ¹⁰⁶, H. Zbroszczyk ¹⁴⁰, M. Zhalov ⁹⁶, X. Zhang ⁶, Y. Zhang ⁶, Z. Zhang ^{6,132}, C. Zhao ²¹,
 V. Zherebchevskii ¹¹¹, N. Zhigareva ⁶⁴, D. Zhou ⁶, Y. Zhou ⁸⁸, Z. Zhou ²², H. Zhu ⁶, J. Zhu ⁶, Y. Zhu ⁶,
 A. Zichichi ^{27,10}, M.B. Zimmermann ³⁴, G. Zinovjev ², J. Zmeskal ¹¹², S. Zou ⁶

¹ A.I. Alikhanyan National Science Laboratory (Yerevan Physics Institute) Foundation, Yerevan, Armenia² Bogolyubov Institute for Theoretical Physics, National Academy of Sciences of Ukraine, Kiev, Ukraine³ Bose Institute, Department of Physics and Centre for Astroparticle Physics and Space Science (CAPSS), Kolkata, India⁴ Budker Institute for Nuclear Physics, Novosibirsk, Russia⁵ California Polytechnic State University, San Luis Obispo, CA, United States⁶ Central China Normal University, Wuhan, China⁷ Centre de Calcul de l'IN2P3, Villeurbanne, Lyon, France⁸ Centro de Aplicaciones Tecnológicas y Desarrollo Nuclear (CEADEN), Havana, Cuba⁹ Centro de Investigación y de Estudios Avanzados (CINVESTAV), Mexico City and Mérida, Mexico¹⁰ Centro Fermi – Museo Storico della Fisica e Centro Studi e Ricerche "Enrico Fermi", Rome, Italy¹¹ Chicago State University, Chicago, IL, United States¹² China Institute of Atomic Energy, Beijing, China¹³ Chonbuk National University, Jeonju, Republic of Korea¹⁴ Comenius University Bratislava, Faculty of Mathematics, Physics and Informatics, Bratislava, Slovakia¹⁵ COMSATS Institute of Information Technology (CIIT), Islamabad, Pakistan¹⁶ Creighton University, Omaha, NE, United States¹⁷ Department of Physics, Aligarh Muslim University, Aligarh, India¹⁸ Department of Physics, Pusan National University, Pusan, Republic of Korea¹⁹ Department of Physics, Sejong University, Seoul, Republic of Korea²⁰ Department of Physics, University of California, Berkeley, CA, United States²¹ Department of Physics, University of Oslo, Oslo, Norway²² Department of Physics and Technology, University of Bergen, Bergen, Norway²³ Dipartimento di Fisica dell'Università 'La Sapienza' and Sezione INFN, Rome, Italy²⁴ Dipartimento di Fisica dell'Università and Sezione INFN, Cagliari, Italy²⁵ Dipartimento di Fisica dell'Università and Sezione INFN, Trieste, Italy²⁶ Dipartimento di Fisica dell'Università and Sezione INFN, Turin, Italy²⁷ Dipartimento di Fisica e Astronomia dell'Università and Sezione INFN, Bologna, Italy²⁸ Dipartimento di Fisica e Astronomia dell'Università and Sezione INFN, Catania, Italy

- ²⁹ Dipartimento di Fisica e Astronomia dell'Università and Sezione INFN, Padova, Italy
³⁰ Dipartimento di Fisica 'E.R. Caianiello' dell'Università and Gruppo Collegato INFN, Salerno, Italy
³¹ Dipartimento DISAT del Politecnico and Sezione INFN, Turin, Italy
³² Dipartimento di Scienze e Innovazione Tecnologica dell'Università del Piemonte Orientale and INFN Sezione di Torino, Alessandria, Italy
³³ Dipartimento Interateneo di Fisica 'M. Merlin' and Sezione INFN, Bari, Italy
³⁴ European Organization for Nuclear Research (CERN), Geneva, Switzerland
³⁵ Faculty of Electrical Engineering, Mechanical Engineering and Naval Architecture, University of Split, Split, Croatia
³⁶ Faculty of Engineering and Science, Western Norway University of Applied Sciences, Bergen, Norway
³⁷ Faculty of Nuclear Sciences and Physical Engineering, Czech Technical University in Prague, Prague, Czech Republic
³⁸ Faculty of Science, P.J. Šafárik University, Košice, Slovakia
³⁹ Frankfurt Institute for Advanced Studies, Johann Wolfgang Goethe-Universität Frankfurt, Frankfurt, Germany
⁴⁰ Gangneung-Wonju National University, Gangneung, Republic of Korea
⁴¹ Gauhati University, Department of Physics, Guwahati, India
⁴² Helmholtz-Institut für Strahlen- und Kernphysik, Rheinische Friedrich-Wilhelms-Universität Bonn, Bonn, Germany
⁴³ Helsinki Institute of Physics (HIP), Helsinki, Finland
⁴⁴ High Energy Physics Group, Universidad Autónoma de Puebla, Puebla, Mexico
⁴⁵ Hiroshima University, Hiroshima, Japan
⁴⁶ Hochschule Worms, Zentrum für Technologietransfer und Telekommunikation (ZTT), Worms, Germany
⁴⁷ Horia Hulubei National Institute of Physics and Nuclear Engineering, Bucharest, Romania
⁴⁸ Indian Institute of Technology Bombay (IIT), Mumbai, India
⁴⁹ Indian Institute of Technology Indore, Indore, India
⁵⁰ Indonesian Institute of Sciences, Jakarta, Indonesia
⁵¹ INFN, Laboratori Nazionali di Frascati, Frascati, Italy
⁵² INFN, Sezione di Bari, Bari, Italy
⁵³ INFN, Sezione di Bologna, Bologna, Italy
⁵⁴ INFN, Sezione di Cagliari, Cagliari, Italy
⁵⁵ INFN, Sezione di Catania, Catania, Italy
⁵⁶ INFN, Sezione di Padova, Padova, Italy
⁵⁷ INFN, Sezione di Roma, Rome, Italy
⁵⁸ INFN, Sezione di Torino, Turin, Italy
⁵⁹ INFN, Sezione di Trieste, Trieste, Italy
⁶⁰ Inha University, Incheon, Republic of Korea
⁶¹ Institut de Physique Nucléaire d'Orsay (IPNO), Institut National de Physique Nucléaire et de Physique des Particules (IN2P3/CNRS), Université de Paris-Sud, Université Paris-Saclay, Orsay, France
⁶² Institute for Nuclear Research, Academy of Sciences, Moscow, Russia
⁶³ Institute for Subatomic Physics, Utrecht University/Nikhef, Utrecht, Netherlands
⁶⁴ Institute for Theoretical and Experimental Physics, Moscow, Russia
⁶⁵ Institute of Experimental Physics, Slovak Academy of Sciences, Košice, Slovakia
⁶⁶ Institute of Physics, Homi Bhabha National Institute, Bhubaneswar, India
⁶⁷ Institute of Physics of the Czech Academy of Sciences, Prague, Czech Republic
⁶⁸ Institute of Space Science (ISS), Bucharest, Romania
⁶⁹ Institut für Kernphysik, Johann Wolfgang Goethe-Universität Frankfurt, Frankfurt, Germany
⁷⁰ Instituto de Ciencias Nucleares, Universidad Nacional Autónoma de México, Mexico City, Mexico
⁷¹ Instituto de Física, Universidade Federal do Rio Grande do Sul (UFRGS), Porto Alegre, Brazil
⁷² Instituto de Física, Universidad Nacional Autónoma de México, Mexico City, Mexico
⁷³ iThemba LABS, National Research Foundation, Somerset West, South Africa
⁷⁴ Johann-Wolfgang-Goethe Universität Frankfurt Institut für Informatik, Fachbereich Informatik und Mathematik, Frankfurt, Germany
⁷⁵ Joint Institute for Nuclear Research (JINR), Dubna, Russia
⁷⁶ Korea Institute of Science and Technology Information, Daejeon, Republic of Korea
⁷⁷ KTO Karatay University, Konya, Turkey
⁷⁸ Laboratoire de Physique Subatomique et de Cosmologie, Université Grenoble-Alpes, CNRS-IN2P3, Grenoble, France
⁷⁹ Lawrence Berkeley National Laboratory, Berkeley, CA, United States
⁸⁰ Lund University Department of Physics, Division of Particle Physics, Lund, Sweden
⁸¹ Nagasaki Institute of Applied Science, Nagasaki, Japan
⁸² Nara Women's University (NWU), Nara, Japan
⁸³ National and Kapodistrian University of Athens, School of Science, Department of Physics, Athens, Greece
⁸⁴ National Centre for Nuclear Research, Warsaw, Poland
⁸⁵ National Institute of Science Education and Research, Homi Bhabha National Institute, Jatni, India
⁸⁶ National Nuclear Research Center, Baku, Azerbaijan
⁸⁷ National Research Centre Kurchatov Institute, Moscow, Russia
⁸⁸ Niels Bohr Institute, University of Copenhagen, Copenhagen, Denmark
⁸⁹ Nikhef, National Institute for Subatomic Physics, Amsterdam, Netherlands
⁹⁰ NRC Kurchatov Institute IHEP, Protvino, Russia
⁹¹ NRNU Moscow Engineering Physics Institute, Moscow, Russia
⁹² Nuclear Physics Group, STFC Daresbury Laboratory, Daresbury, United Kingdom
⁹³ Nuclear Physics Institute of the Czech Academy of Sciences, Řež u Prahy, Czech Republic
⁹⁴ Oak Ridge National Laboratory, Oak Ridge, TN, United States
⁹⁵ Ohio State University, Columbus, OH, United States
⁹⁶ Petersburg Nuclear Physics Institute, Gatchina, Russia
⁹⁷ Physics Department, Faculty of science, University of Zagreb, Zagreb, Croatia
⁹⁸ Physics Department, Panjab University, Chandigarh, India
⁹⁹ Physics Department, University of Jammu, Jammu, India
¹⁰⁰ Physics Department, University of Rajasthan, Jaipur, India
¹⁰¹ Physikalisches Institut, Eberhard-Karls-Universität Tübingen, Tübingen, Germany
¹⁰² Physikalisches Institut, Ruprecht-Karls-Universität Heidelberg, Heidelberg, Germany
¹⁰³ Physik Department, Technische Universität München, Munich, Germany
¹⁰⁴ Research Division and ExtreMe Matter Institute EMMI, GSI Helmholtzzentrum für Schwerionenforschung GmbH, Darmstadt, Germany
¹⁰⁵ Rudjer Bošković Institute, Zagreb, Croatia
¹⁰⁶ Russian Federal Nuclear Center (VNIIEF), Sarov, Russia

- 107 Saha Institute of Nuclear Physics, Homi Bhabha National Institute, Kolkata, India
108 School of Physics and Astronomy, University of Birmingham, Birmingham, United Kingdom
109 Sección Física, Departamento de Ciencias, Pontificia Universidad Católica del Perú, Lima, Peru
110 Shanghai Institute of Applied Physics, Shanghai, China
111 St. Petersburg State University, St. Petersburg, Russia
112 Stefan Meyer Institut für Subatomare Physik (SMI), Vienna, Austria
113 SUBATECH, IMT Atlantique, Université de Nantes, CNRS-IN2P3, Nantes, France
114 Suranaree University of Technology, Nakhon Ratchasima, Thailand
115 Technical University of Košice, Košice, Slovakia
116 Technische Universität München, Excellence Cluster 'Universe', Munich, Germany
117 The Henryk Niewodniczanski Institute of Nuclear Physics, Polish Academy of Sciences, Cracow, Poland
118 The University of Texas at Austin, Austin, TX, United States
119 Universidad Autónoma de Sinaloa, Culiacán, Mexico
120 Universidade de São Paulo (USP), São Paulo, Brazil
121 Universidade Estadual de Campinas (UNICAMP), Campinas, Brazil
122 Universidade Federal do ABC, Santo André, Brazil
123 University College of Southeast Norway, Tønsberg, Norway
124 University of Cape Town, Cape Town, South Africa
125 University of Houston, Houston, TX, United States
126 University of Jyväskylä, Jyväskylä, Finland
127 University of Liverpool, Liverpool, United Kingdom
128 University of Tennessee, Knoxville, TN, United States
129 University of the Witwatersrand, Johannesburg, South Africa
130 University of Tokyo, Tokyo, Japan
131 University of Tsukuba, Tsukuba, Japan
132 Université Clermont Auvergne, CNRS/IN2P3, LPC, Clermont-Ferrand, France
133 Université de Lyon, Université Lyon 1, CNRS/IN2P3, IPN-Lyon, Villeurbanne, Lyon, France
134 Université de Strasbourg, CNRS, IPHC UMR 7178, F-67000 Strasbourg, France, Strasbourg, France
135 Université Paris-Saclay Centre d'études de Saclay (CEA), IRFU, Department de Physique Nucléaire (DPhN), Saclay, France
136 Università degli Studi di Foggia, Foggia, Italy
137 Università degli Studi di Pavia, Pavia, Italy
138 Università di Brescia, Brescia, Italy
139 Variable Energy Cyclotron Centre, Homi Bhabha National Institute, Kolkata, India
140 Warsaw University of Technology, Warsaw, Poland
141 Wayne State University, Detroit, MI, United States
142 Westfälische Wilhelms-Universität Münster, Institut für Kernphysik, Münster, Germany
143 Wigner Research Centre for Physics, Hungarian Academy of Sciences, Budapest, Hungary
144 Yale University, New Haven, CT, United States
145 Yonsei University, Seoul, Republic of Korea

i Deceased.

ii Dipartimento DET del Politecnico di Torino, Turin, Italy.

iii M.V. Lomonosov Moscow State University, D.V. Skobeltsyn Institute of Nuclear, Physics, Moscow, Russia.

iv Department of Applied Physics, Aligarh Muslim University, Aligarh, India.

v Institute of Theoretical Physics, University of Wroclaw, Poland.